nature photonics

SUPPLEMENTARY INFORMATION

DOI: 10.1038/NPHOTON.2015.124

Characterization of Tandem Organic Solar Cells

Ronny Timmreck[1], Toni Meyer[1], Jan Gilot[2], Holger Seifert[3], Toni Mueller[4], Alice Furlan[5], Martijn M. Wienk[5], David Wynands[1,6], Jochen Hohl-Ebinger[3] , Wilhelm Warta[3], René A.J. Janssen[5], Moritz Riede[1,7], Karl Leo[1]

[1]Institut für Angewandte Photophysik, Technische Universität Dresden (TUD), 01062 Dresden, Germany

[2]Holst Centre, High Tech Campus 31, 5656 AE, Eindhoven, The Netherlands

[3]Fraunhofer ISE, Fraunhofer Institute for Solar Energy Systems (ISE), Heidenhofstr. 2, 79110 Freiburg, Germany

[4]Heliatek GmbH, Treidlerstr. 3, 01139 Dresden, Germany

[5]Molecular Materials and Nanosystems, Eindhoven University of Technology (TUe), 5600 MB Eindhoven, Netherlands

[6]Present address: Fraunhofer COMEDD, Maria-Reiche-Straße 2, 01109 Dresden, Germany

[7]Present address: Clarendon Laboratory, Physics Department, University of Oxford, Parks Road, Oxford OX1 3PU England, UK

Contents

1 Introduction

Among the various thin-film photovoltaics (PV) technologies, organic photovoltaics (OPV) as all-carbon technology has great potential due to low cost production, flexibility, semitransparency, light weight, and tunable color.

However, to achieve competitive efficiencies around 15% or more, OPV will necessitate tandem or even triple junction approaches. An efficient realization of such multijunction cells is difficult, so that the record efficiency for tandem cells of 10.6%[1] is still slightly behind the record for single-junction organic solar cells with 11.1%[2] efficiency. However, the number of publications with topics covering tandem OPV has rapidly increased over the last years. From 2004 to 2014, the number of publications dealing with tandem organic solar cells increased from less than 25

DOI: 10.1038/NPHOTON.2015.124

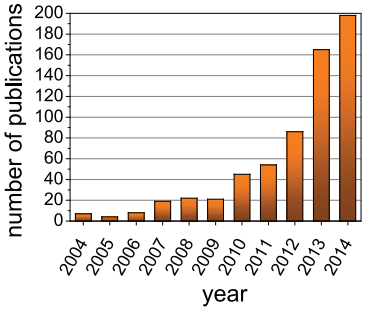

Fig. S1: *Number of publications being found with the keywords "TOPIC: tandem AND (organic OR polymer) AND (solar cell OR photovoltaic)" from Web of Science™ from 2004 to 2014.*

Quality of tandem organic solar cell characterization	number of publications	percentage	References
according to standard[3]	3	4%	[1,4,5]
EQE for the subcells shown (not only dummy single cells) No comment on mismatch factor M or M not used for characterization	33	45%	[6–39]
No EQE for subcells shown No comment on M	37	51%	[40–75]

Tab. S1: *Analysis of the publication practice of tandem organic solar cell efficiencies in selected publications in Web of Science™. The analysis is mainly based on a search with the keywords "TITLE: (tandem AND (organic OR polymer) AND (solar cell or photovoltaic)) AND YEAR PUBLISHED: (2009-2014)". Review papers and papers where the tandem organic solar cell efficiency characterization is not in the focus of the work as well as papers only showing simulation results are not shown. The total number of analyzed papers is 73.*

to almost 200 a year (see Fig. S1). Nevertheless, the literature survey presented in the main text shows that the quality of tandem OPV characterization does not reflect its great potential. In addition to Table 1 of the main text, Table S1 presents the complete list of references of this literature survey.

It should be mentioned that even though publications [1,5] present results measured in full accordance to the applicable standards their conclusions about the necessity of a bias-voltage for SR measurement are possibly incorrect. The reason is that the bias voltage for SR measurements having only little influence on the measurement of inorganic solar cell is a crucial parameter for organic tandem solar cells as described in detail in subsection 3.1 of this supplementary information.

2 Measurement standards and procedures for the characterization of tandem solar cells

The main task when measuring solar cells - not only tandem solar cells - is to assure standard reporting conditions (SRC) which means measuring at 25 °C (junction temperature), illumination intensity of 1000 W/m² with an AM1.5g spectrum[76]. These reporting conditions apply to terrestrial use of non-concentrating solar cells. For other applications such as operation in space (AM0, 1367 W/m²)[77] or concentrating solar devices (AM1.5d, 1000 W/m²)[78,79], different reporting conditions have to be used. Temperature and illumination density are parameters that can be controlled relatively easily. In contrast, a full control of the illumination spectrum is experimentally impossible with light sources available at present.

For single solar cells, the concept of spectral mismatch correction as described in standard IEC 60904-7[80] or ASTM E973[81] has to be applied by taking the spectral mismatch factor M into account[82]. The aim of this procedure is to assure that the solar cell under test generates the same number of charge carriers as it would generate under the AM1.5g spectrum. One needs a solar simulator according to the standards IEC 60904-9[83] or ASTM E 927[84] and the spectral distribution of the solar simulator needs to be determined by a spectroradiometer. It should be noted that the spectrum varies with set intensity, aging of light sources, and optical components of the simulator such as filters. Thus, a manufacturer's data of the spectral distribution might differ from the actual irradiance and should be checked regularly.

A solar cell spectrally weights an irradiation according to its spectral response (SR) $s(\lambda)$. As the illumination spectrum of any solar simulator differs from the standard spectrum, the device under test will weight the irradiation differently. Thus, the SR of the solar cell under test needs to be determined as referred to in section 3.1. To set the total irradiance of the solar simulator, a calibrated reference cell is used. Perfectly matched reference cells are not at hand, especially for organic photovoltaics, meaning the SR of the reference cell differs from that one under test. Hence, spectra are weighted differently. Therefore, the SR of the reference cell needs to be known and used for the computation of the mismatch factor M.

The determination of the current density-voltage characteristics (JV-characteristics) itself is carried out according to standards IEC 60904-1[85] or ASTM E948[86]. For organic solar cells, where a non-linearity of the current dependent on the light intensity is expected as shown later, a setting of the solar simulator to effective irradiances, as described in IEC 60904-7[80], is preferred to recalculating the measured JV-characteristics to the desired effective irradiance.

For tandem solar cell devices, or multi-junction solar cells in general, the procedure of spectral mismatch correction is more complicated. Tandem solar cells consist of two individual solar cells (denoted as subcells). Therefore, the correction of the spectral mismatch has to be done with the condition that for each subcell, the number of generated charge carriers is equal under test and reference spectrum. This can in general only be achieved with a spectrally tunable solar simulator with at least as many individually adjustable light sources as subcells in the multi-junction device under test.[3] By correcting the spectral mismatch of one of the subcells, the other subcells are influenced in general. Therefore the measurement procedure as given by the appropriate ASTM standard E 2236[3] is iterative. After measuring the spectral distribution of the solar simulator by a spectroradiometer, the mismatch factors for both subcells are determined, the short circuit currents of the reference cell(s) are measured, and the current balances are calculated. These are defined for each subcell i as

$$Z_i = \frac{1}{M_i} \frac{E_{SRC} C^{RC}}{I_{SIM}^{RC}}, \tag{1}$$

where M_i is the mismatch factor according to the actual simulator spectrum, the reference cell and the subcell i. E_{SRC} is the total irradiance of the standard spectrum, C^{RC} the calibration value of the reference cell and I_{SIM}^{RC} its current at the simulator irradiance.

If the current balances for each cell deviate too far from unity, the light sources need to be readjusted and the procedure needs to be repeated. The procedure is therefore time-consuming and not very handy. In reference[3] constraints of the current balances are given by 3 % for reasonable limits, for minimal spectral errors by 1 %. Especially in the case of organic tandem solar cells with a considerable spectral mismatch between test- and reference cell, these constraints are somewhat artificial. Due to their spectral properties, organic solar cells might be more sensitive to spectral variations than inorganic multi-junction devices. Hence, one should determine the dependence of the actual device under test to spectral variations in order to achieve the desired accuracy. Since spectrally adjustable sun simulators are not at hand in many research labs, section 7.3 of ASTM E2236[3] ("Electrical Performance, non-spectrally adjustable Light Source") also suggests an alternative procedure involving the use of a non-spectrally adjustable light source. According to that, the mismatch factor of the subcell limiting the current under the reference spectrum should be used for calibration. It will be investigated in the following sections whether this procedure is applicable to tandem organic solar cells.

DOI: 10.1038/NPHOTON.2015.124

Since the iterative procedure of ASTM E2236 using a spectrally adjustable solar simulator is time-consuming and inconvenient, Meusel et al. proposed an alternative measurement procedure being much faster[87], but with results being equal to those achieved by using the procedure as given by ASTM E2236. According to reference [87] one can calculate the photocurrent densities of each subcell under the reference spectrum as well as under the simulator spectrum J_{top}^{ref}, J_{bot}^{ref}, J_{top}^{sim} and J_{bot}^{sim}. The subcells are denoted top and bottom cell with top being hit first by the incident light. The required quantities for this calculation are the relative external quantum efficiencies of top and bottom cell that can be converted into relative spectral responses s_{top} and s_{bot}, the relative spectra with fixed spectral distribution of the two light sources e_1 and e_2 of a multi-source sun simulator forming the spectrally adjustable solar simulator, the reference spectrum E_{ref}, that is usually the AM1.5g reference spectrum, as well as the certified absolute spectral response of the reference cell S_{RC}.

Because both subcells should generate the same current during the experiment as under the reference spectrum, J_{top}^{ref} has to equal J_{top}^{sim} and J_{bot}^{ref} has to equal J_{bot}^{sim} at the same time.

The result of the complete derivation is a two-dimensional, inhomogeneous system of linear equations with two unknown parameters A_1 and A_2 representing the intensities of the two light sources of a multi-source sun simulator:

$$A_1 \int s_{top}(\lambda)e_1(\lambda)d\lambda + A_2 \int s_{top}(\lambda)e_2(\lambda)d\lambda = \int s_{top}(\lambda)E_{ref}(\lambda)d\lambda \tag{2}$$

$$A_1 \int s_{bot}(\lambda)e_1(\lambda)d\lambda + A_2 \int s_{bot}(\lambda)e_2(\lambda)d\lambda = \int s_{bot}(\lambda)E_{ref}(\lambda)d\lambda\,. \tag{3}$$

Using these parameters achieved by solving the system of equations, J_{sc} of the reference cell under solely light source 1 J_{RC}^1 as well as under solely light source 2 J_{RC}^2 of the multi-source sun simulator can be calculated allowing their individual calibration[87]:

$$J_{RC}^1 = A_1 \int S_{RC}(\lambda)e_1(\lambda)d\lambda \tag{4}$$

$$J_{RC}^2 = A_2 \int S_{RC}(\lambda)e_2(\lambda)d\lambda\,. \tag{5}$$

Getting both light sources calibrated in such a way to the test cell simultaneously assures that both subcells exhibit the same J_{sc} as under AM1.5g, i.e. simultaneous mismatch correction of both subcells is achieved. Since it is a comparably fast procedure to set the spectral irradiance to certain conditions, methods investigating the dependence of the spectral irradiance such as the spectrometric characterization become more applicable. According to reference[87], in the spectrometric characterization method the multi-dimensional space of all illumination spectra is mapped on a two dimensional vector space of positive real numbers. Each single possible illumination spectrum $E(\lambda)$ is represented by a point $(G_{eff}^{top}, G_{eff}^{bot}) \in \mathbb{R}_+^2$. Here, G_{eff}^{top} and G_{eff}^{bot} are the effective irradiances[87] of a spectrum $E(\lambda)$ on the two subcells. These effective irradiances are proportional to the generated charge carrier densities of the subcells. Since in a tandem solar cell, the current densities of both subcells have to be the same, the dimensionality of the problem can be reduced to a line in two dimensional space - the so called 'line of measurement'. Each point on this 'line of measurement' can be specified by the parameter Z, such that $(1+Z, 1-Z)$ represents a particular spectrum and therefore a particular multi-source sun simulator setting. The corresponding parameters A_1 and A_2 can be calculated depending on Z as follows:

$$A_1 \int s_{top}(\lambda)e_1(\lambda)d\lambda + A_2 \int s_{top}(\lambda)e_2(\lambda)d\lambda = (1+Z) \int s_{top}(\lambda)E_{ref}(\lambda)d\lambda \tag{6}$$

$$A_1 \int s_{bot}(\lambda)e_1(\lambda)d\lambda + A_2 \int s_{bot}(\lambda)e_2(\lambda)d\lambda = (1-Z) \int s_{bot}(\lambda)E_{ref}(\lambda)d\lambda\,. \tag{7}$$

The spectrum at $Z = 0$ is the chosen reference spectrum. The formalism of spectrometric characterization allows the calculation of the particular intensities of each light source to reach a specific

point $(1+Z, 1-Z)$ and thereby a specific spectrum. It is noted that the effective irradiance for all spectra on the 'line of measurement' equals almost that of the used reference spectrum. Consequently, it is not possible to aim for a specific spectrum at a specific irradiance in one characterization cycle. To estimate the parameters of the tandem solar cell for spectra differing from the reference spectrum, e.g. for estimating the changes in efficiency over one day due to variations of air mass, the values at the respective point on the 'line of measurement' have to be scaled requiring their linear behavior for validity. It should be noted that this method allows to estimate the spectral dependence of the solar cell under test but is misleading in terms of characterization according to the standards. To achieve precise results, the spectrum of interest has to be used as standard spectrum in the parameter calculation (equations 2 and 3).

The mentioned standards as well as the spectrometric characterization method were developed for inorganic tandem solar cells. They do not consider the special characteristics of organic solar cells. Therefore, in the next section of this paper, properties distinguishing organic tandem solar cells from inorganic ones that influence the measurement procedure are discussed.

3 Characterization of tandem organic solar cells

3.1 Spectral Response measurement

Theory and measurement procedures

The first step in characterizing solar cells should be a spectral response (SR) measurement whether single or multi-junction solar cell. With the result of this method, it is possible to determine the spectral mismatch of single junction solar cells to calculate the intensity of the light source for calibration. In the case of multi-junction solar cells the spectral mismatch of each subcell can be determined and hence the intensity of the light sources to apply a specific spectrum on the tandem solar cell. In most cases, this is the only objective and therefore a relative SR spectrum $s(\lambda)$ is sufficient. Absolute SR spectra $S(\lambda)$ are only required if the j_{sc} of the subcells of the tandem cell have to be correctly estimated by convoluting SR and AM1.5g solar spectrum. While the SR represents the spectrally resolved ratio of generated current to irradiated power, the often used quantity external quantum efficiency (EQE) represents the ratio of extracted charges to irradiated photons. From the spectral response one can calculate the EQE as follows:

$$EQE(\lambda) = \frac{S(\lambda)}{\lambda}\frac{hc}{e}\,. \tag{8}$$

In a tandem solar cell with serial connected subcells, a standard SR-measurement tracing the electrical response of the solar cell to a continuous variable monochromatic light beam, cannot lead to a reasonable result. In this case, only the response of the subcell that is limiting the current at this particular wavelength is measured. Apart from artifacts, the result of such a measurement is therefore the lower envelope of the spectral responses of both subcells which normally has no practical meaning. However, from the comparison to the SR of the subcells, further conclusions about the quality of the measurement can be drawn as will be shown later.

To correctly measure the spectral response of one of the subcells, a bias light has to be selected in a way that independently of the wavelength of the monochromatic probe light, the subcell not to be measured, hereafter denoted as optically biased subcell, generates more current than the subcell to be measured. In general, the choice of the bias light spectrum can be based on the absorption profile of the absorber materials or the individually measured spectral response of single junction solar cells, comprising the same absorber material as the subcells of the tandem cell. This is an appropriate method when the absorption profile of the active materials does not show significant overlap[4,88]. If both subcells comprise strongly spectrally overlapping or even the same absorber materials, which can be advantageous for particular absorber materials[31], detailed optical simulations of the tandem solar cell stack have to be carried out to decide for appropriate bias light spectra (cp. section 3.4). A detailed study how to treat such devices concerning bias light selection can be found in reference [89].

DOI: 10.1038/NPHOTON.2015.124

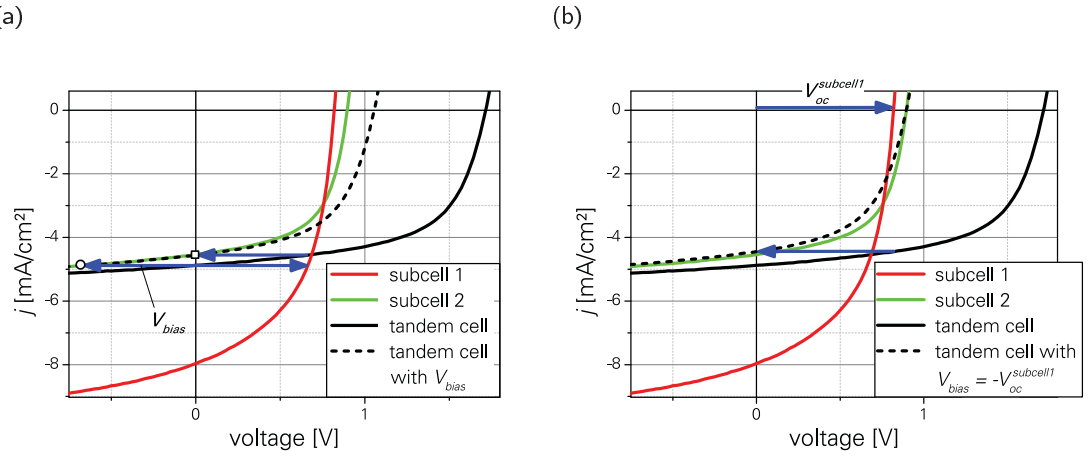

Fig. S2: *Schematic description of the JV-characteristics of a tandem organic solar cell and its subcells. While measuring spectral response of subcell 2 without applying a bias voltage, the tandem cell is at short-circuit, but subcell 2 is at reverse bias (circular symbol). The resulting spectral response will be overestimated. a) By applying a bias voltage V_{bias} the JV-characteristics of the tandem cell is moved towards more negative voltages (dashed curve) such that subcell 2 will be at short-circuit condition (squared symbol) as it is necessary for a correct spectral response measurement. (b) Since V_{bias} is hard to determine, an easy approximation is to use $V_{oc}^{subcell1}$ as bias voltage. This leads to slight deviations compared to using V_{bias}.*

As described above, a tandem solar cell has to be illuminated with a continuous bias light in every case. Therefore, the monochromatic probe light has to be chopped and the current response of the solar cell analyzed using lock-In technique in order to detect only the current signal originating from the probe light but not from the bias light.

When the tandem solar cell is illuminated by a bias light matching the absorption of one of the subcells such that this subcell is generating much more charge carriers than the other subcell, this subcell will operate close to its open-circuit voltage ($V_{oc}^{subcell1}$). Thus, the current-limiting subcell the SR of which will be measured operates under reverse bias when the tandem solar cell is at short-circuit conditions (cp. Fig. S2). As discussed in the main text, organic solar cells often suffer from low fill factors or even photoinduced shunts. As a consequence, the photocurrent of the measured subcell detected while the tandem solar cell is at short-circuit conditions, will be overestimated. Hence, the SR will also be overestimated. This overestimation can be compensated for by applying a forward electrical bias that moves the JV-characteristics of the tandem cell towards more negative voltages, such that the j_{sc} of the tandem cell equals the j_{sc} of the subcell under test. Fig. S2 schematically shows the result of a bias voltage application. Since the j_{sc} of the subcells are unknown in general an approximation has to be made.

If the bias light intensity is sufficiently high, the optically biased subcell is working close to its V_{oc} at this illumination conditions, regardless of the voltage of the whole tandem solar cell. Hence, a possible approximation to get the subcell to be tested to short-circuit conditions is to apply a voltage equaling the V_{oc} of the optically biased subcell (Fig. S2(b)). However, depending on the FF of the subcells and the intensity of the bias light, the error compared to a measurement under exact bias voltage V_{bias} (cp. Fig. S2a)) can be substantial[90]. To avoid this error, bias voltage determination has to be done carefully, e.g. according to the procedure given in reference[90]. There, single cells similar to the subcells of the tandem cell in terms of absorber materials as well as charge carrier generation rate (dummy cells) are used. The illumination is chosen exactly as during the SR-measurement: the dummy cell corresponding to the optically biased subcell is exposed to the bias light and the dummy cell corresponding to the subcell under test is illuminated by the monochromatic probe light. Because the monochromatic probe light in general varies in

intensity, the procedure involves measurements at the wavelengths with its minimum and maximum intensity. The current density value in the JV-characteristics of the dummy cells, where the sum of the voltages of both cells is zero, equals the short circuit point in the tandem solar cell. The corresponding voltage of the dummy cell exposed to the bias light is the bias voltage that has to be used for the SR-measurement. Normally, it is sufficient to use the average of the voltage values resulting from the different monochromatic light intensities. A detailed description of the the procedure can be found in reference[90].

It has to be noted that it is in general impossible to draw conclusion about the necessary bias voltage for SR measurement from JV-measurements under dark conditions since the slope of the $J_{dark}V$-curve around $V = 0$ can significantly differ from its value of the $J_{photo}V$-curve. The reason is that the slope of the $J_{photo}V$-curve around $V = 0$ is in general not mainly determined by the shunt resistances of the device as it is true for inorganic solar cells but by other fill factor dominating effects. Such effects are for instance bimolecular recombination, field-dependent charge extraction or generation, hampered charge extraction as well as poor selectivity of the contacts. In contrast, most of these effects do not influence the shape of the $J_{dark}V$-curve such that it is in general virtually flat around $V = 0$. The calculation of the shunt resistance from $J_{dark}V$-curves as done in references [1,5] is therefore not a reasonable approach for organic tandem solar cells.

Furthermore, ASTM standard E 2236 demands for a flood light, making sure that the subcell under test is illuminated with an intensity similar to one sun or at least some illumination, because the spectral responsivities of the device can be a function of the illumination level[3]. However, the overall charge carrier generation in the subcell under test has to be lower than that of the optically biased subcell.

Using lock-in technique, the non-differential spectral response $s(\lambda)$ is inaccessible directly in this kind of measurement. Only the slope of the monochromatically generated j_{sc} versus irradiance E, the so called differential spectral response $\tilde{s}(\lambda)$, can be measured[91].

$$\tilde{s}(\lambda, j_{sc}(E_b)) = \frac{\partial j_{sc}(E_{bias})}{\partial E(\lambda)} \tag{9}$$

$s(\lambda)$ only equals to $\tilde{s}(\lambda)$ if the photocurrent of the measured subcell depends linearly on light intensity. This, however, is not the case for organic solar cells in general. To calculate the spectral mismatch factor, or in the case of tandem solar cells to calculate the parameters for spectral correction, $s(\lambda)$ has to be calculated from the measured $\tilde{s}(\lambda)$. For single solar cells, this can be done according to reference[92] where $\tilde{s}(\lambda)$ is measured as a function of the short circuit current density j_{sc} over a range of bias intensities E_{bias}. The (non-differential) spectral response $s(\lambda)$ at standard reporting condition can be calculated as follows:

$$s_{STC}(\lambda) = \frac{J_{SRC}}{\int_0^{J_{STC}} \frac{dJ_{bias}}{\tilde{s}(\lambda, J_{bias})}} . \tag{10}$$

For this method, the measurement of the short circuit current density at different bias light intensities is necessary. Because the short circuit current of each individual subcell is inaccessible, the method is not applicable for tandem solar cells. An alternative procedure using scaling factors for the SR is demonstrated in reference [93]. However, it is also only demonstrated for single solar cells. Hence, for tandem organic solar cells the difference between the differential and non-differential spectral responsivity has not been taken into consideration up to now. It should be noted that neglecting the difference of differential and non-differential spectral response can lead to incorrect characterization results. Therefore, efforts should be made to find methods for determining the non-differential spectral response of tandem solar cells.

Experiments

SR-measurements according to the described standards and procedures have been carried out on tandem solar cell sample A (see Fig. S3 for layer stack). The bias voltage applied across the tandem solar cell was 0.9V and 0.81V for the red and green absorbing subcell, respectively, being approximately the V_{oc} of single cells comprising the same absorber materials.[94,95] In Fig. S4a)

DOI: 10.1038/NPHOTON.2015.124

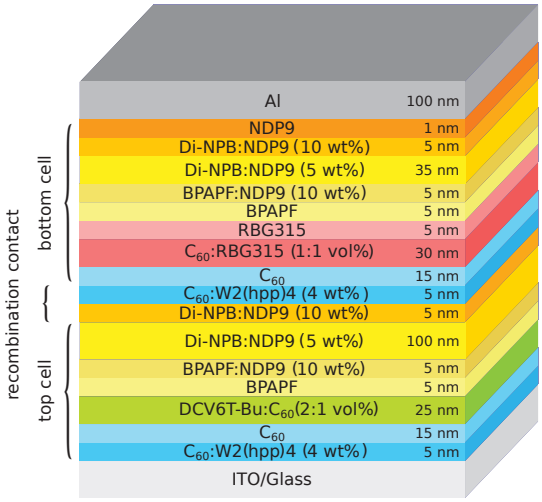

Fig. S3: *Solar cell stack A shown in the order of processing. The green absorbing subcell is facing towards incident light and therefore denoted as as top cell whereas the red absorbing subcell being next to the metal back contact is denoted as bottom cell.*

the *EQE* results of all three participating labs are shown and in Table S2 the j_{sc} calculated by integrating the product of *EQE* and AM1.5g over the wavelength. For red bias light, the only significant deviations can be found in the UV region below 400nm that can be attributed to a degradation of the test cell. While the measurements at TUD and TUe were carried out within a few days, the ISE measurement was performed a few months later. However, due to the low irradiance of the AM1.5g spectrum in this wavelength region, the difference of the integrated photocurrent between 300 and 450 nm is below 0.2 mA/cm^2 for all three measurements. For green bias light, i.e. measuring the red absorbing subcell, the overall deviations are higher but as Fig. S4(b) shows, the normalized *EQE* spectra coincide almost perfectly. The deviations are therefore attributed to non-identical bias light conditions since all three labs use bias light sources of different spectra and intensity. Assuming the SR results are relative, the presented data shows that all three labs achieved equivalent results by using the described measurement procedures. However, the relative differences in the results clearly show that even with great effort, it is hardly possible to achieve absolute spectral responses for tandem organic solar cells. Fortunately, absolute SR values are not required for accurate efficiency determination.

Furthermore, the *EQE* measured without bias illumination exactly follows the lower envelope of the *EQE*-spectra measured with bias light (cp. Fig. S4). This result suggests that leakage paths in this tandem solar cell are low. If the SR measured without bias illumination were higher than these of the subcells, the respective subcell would suffers from a leakage path. Furthermore, this is a confirmation that bias light selection was correct and in each case the intended subcell has been measured.

3.2 *JV*-Characterization and efficiency determination

Theory and Measurement procedures

As already stressed in section 2 the determination of accurate *JV*-characteristics of multi-junction organic solar cell and consequently its efficiency needs to be performed at standard reporting conditions which is only possible by using a spectrally adjustable solar simulator.

If no spectrally adjustable solar simulator is available, the standard ASTM E2236 states an alternative procedure, which however has severe drawbacks for organic solar cells that need to be carefully considered. According to section 7.3 of ASTM E2236 in this case the correction of the spectral mismatch has to be done for the subcell limiting the current under E_{ref}, similar to

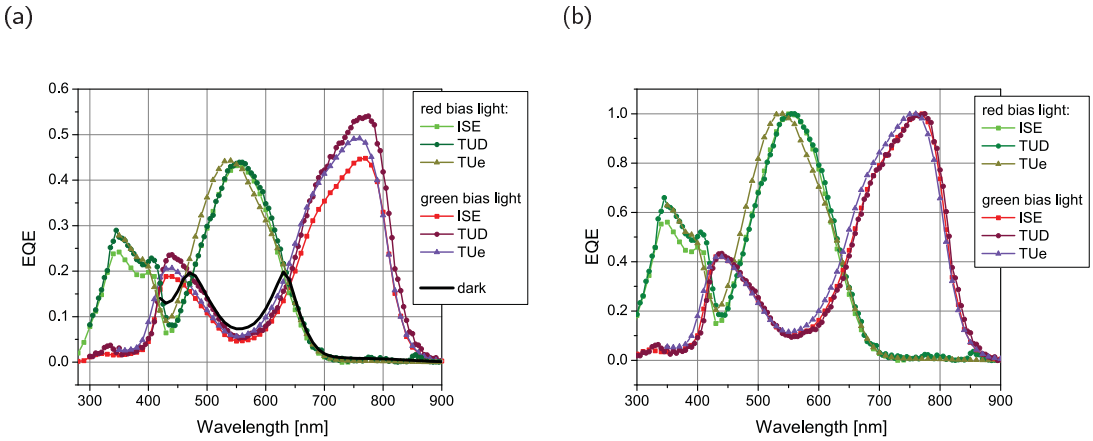

Fig. S4: *(a) Results of the SR-measurements at Fraunhofer-ISE Freiburg (ISE), University of Technology Dresden (TUD) and Eindhoven University of Technology (TUe) and (b) the same spectra normalized to show their relative deviations. The 10 nm shift in the EQE spectra measured at TUe is attributed to a relatively large bandwidth setting of the monochromator, in combination with a small misalignment of the probe beam during the day of this particular measurement.*

the mismatch correction procedure of single junction solar cells. Two main challenges to achieve correct results with this method are identified: Firstly, one needs to assure that the current limiting junction at the specific irradiance is the same one as at the irradiance of SRC. If this is not the case a different simulator has to be used. For a reliable determination of the current limiting subcell, the absolute spectral responses of the subcells would be needed or one needs to assure that all relative spectral responses have the same wavelength independent scaling factor. In the likely case of different nonlinear behavior of the subcells, this conditions cannot be met. In the case of tandem organic solar cells with reasonably current-matched subcells, it is therefore impossible to clearly determine the current limiting subcell while illuminating the tandem cell with a single-source sun simulator.

Secondly, if the spectrum of the used solar simulator does not coincidentally match the AM1.5g spectrum, the effective irradiance of the non-limiting subcell will always be higher than under SRC. The reason for that is the necessary increase of the irradiance of the current limiting subcell to reach calibration in terms of j_{sc}. The result will be that the current-limiting subcell exhibits nearly the j_{sc} of the tandem solar cell under AM1.5g as the overall tandem solar cell will do. Nevertheless, there is excess current in the other junction. This generation is typically leading to a different voltage of the non-limiting subcell compared to SRC. Since the JV-characteristics of the serial connected multi-junction devices are the sum of the voltages of the subcells at equal currents, this excess current in the non-limiting subcell influences the shape of the JV-characteristics of the tandem solar cell. Hence, the fill factor will generally differ from its value at SRC as the efficiency will do.

Experiments

To emphasize the described problems, JV-measurements on device A are carried out with a single source sun simulator at TUD. To calculate the potentially current limiting subcell as preparation for the measurement, the SR data shown in Fig. S4 are multiplied with the simulator spectrum used for the JV-measurement as well as with the AM1.5g reference spectrum for comparison and integrated. The results are shown in Table S2. The calculated j_{sc}-values of the green absorbing subcell (top cell) are at least 20% lower than that of the red absorbing subcell (bottom cell). This clearly indicates that the green absorbing subcell will be current limiting under the reference

DOI: 10.1038/NPHOTON.2015.124

	Top cell (green absorbing)		Bottom cell (red absorbing)	
	j_{sc} at AM1.5g [mA/cm²]	j_{sc} at sun simulator [mA/cm²]	j_{sc} at AM1.5g [mA/cm²]	j_{sc} at sun simulator [mA/cm²]
ISE	4.7	4.9	5.8	6.2
TUe	5.0	5.4	6.6	7.0
TUD	5.1	5.3	7.2	8.1
From absolute *EQE*	4.7		5.5	

Tab. S2: *j_{sc} of the subcells of device A calculated from spectral response data of the three testing institutes shown in Fig. S4 for the AM1.5g reference spectrum as well as the sun simulator spectrum used for JV-characterization. The j_{sc} calculated from the absolute EQE spectra determined by spectrometric characterization as described in subsection 3.3 are shown, too.*

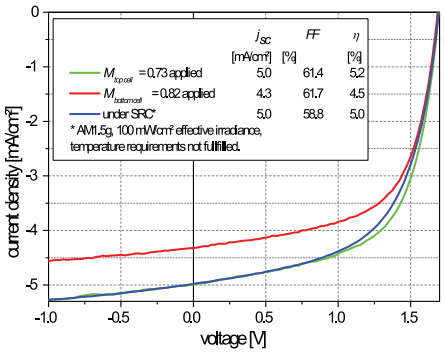

Fig. S5: *Results of JV-measurements on sample A with a single-source sun simulator with applied mismatch factors of bottom (red absorbing) as well as top cell (green absorbing) . For comparison the results of a calibrated JV-measurement under AM1.5g illumination conditions with an effective irradiance of 100mW/cm² on both subcells is shown. The calibration is done according to Meusel et al.[87] using a multi-source sun simulator. The measurements were performed at TUD.*

spectrum as well as under the simulator spectrum. It is very unlikely that different nonlinear behavior of both subcells can lead to relative differences between the SR of the subcells higher than 20%. This assumption will later be validated by the measurement results.

The JV-measurement that is carried out following section 7.3 of ASTM E2236[3] using the mismatch factors of both subcells is shown in Fig. S5. In addition, the result of a JV-measurement under SRC using the calibration method according to Meusel et al.[96] such that the effective irradiance on both subcells is 100mW/cm² is depicted there. For experimental reasons, the temperature requirement of the SRC could not be fulfilled. As the absolute radiation power to the measurement setup is below 100mW, the temperature of the sample can be assumed to be below 35°C during the whole measurement process. According to typical temperature dependencies of small molecule comparable organic solar cells[4], the error in efficiency caused by the increased temperature is small.

Compared to the values under SRC, the application of the mismatch factor of the current limiting subcell results in the correct j_{sc} but in significantly increased fill factor and efficiency values. While the fill factor is 5% too high, the efficiency is overestimated by 4%. Both percentage values are relative to the values under SRC. These findings clearly indicate that a measurement procedure using only a single source sun simulator as given in section 7.3 of standard ASTM E2236 should not be applied to tandem organic solar cells without great care.

In addition to the spectrally corrected JV-measurement shown in Fig. S5, a full spectrometric

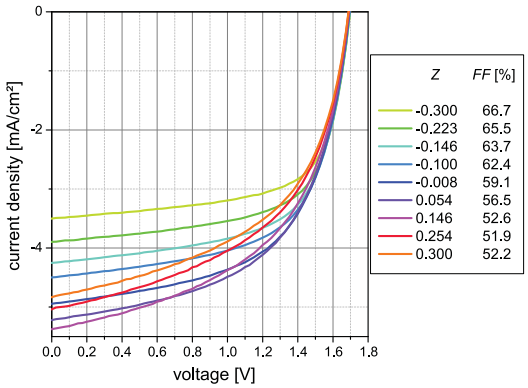

Fig. S6: *Selected JV-characteristics under different illumination spectra (identified by the parameter Z) being the basis for the spectrometric characterization shown in Fig. S7. One can clearly notice the change in fill factor for different spectra due to the influence of the subcells.*

characterization according to Meusel et al.[96] as described in subsection 2 is carried out. For each value of Z, the JV-characteristics are measured and for selected values of Z, they are depicted in Fig. S6. Since the fill factor depends asymmetrically on Z, one can conclude that the subcells exhibit differing fill factors. Furthermore, it is noted that there are no significant deviations of the calculated measurement parameters when using the three different spectral response results depicted in Fig. S4.

The characteristic values of sample A depending on Z measured at TUD as well as ISE are depicted in Fig. S7. At both institutes, the JV-measurements underlying the spectral metrics were measured without aperture leading to differing absolute current values that can be attributed to varying beam divergences of the illumination sources used at both setups. Therefore, the values of ISE are scaled using another effective solar cell area for calculating current densities for reasons of comparability. This way, current density exhibits the same value at AM1.5g as the measurement at TUD. It should be noted, that the determination of the correct effective solar cell area is a crucial issue for the efficiency determination since errors in the order of magnitude of 10%[97] are possible. Because in this article the main focus is on the spectral dependence of the characterization and especially tandem solar cell specific issues, it is referred to the respective literature for the correct treatment of area related challenges[97–101]. Nevertheless, the absolute values of current density and efficiency given in this paper cannot be considered as fully complying to the standards. However, the results of the spectrometric characterization carried out at ISE and TUD qualitatively almost perfectly coincide suggesting correct spectral measurement conditions for the tandem solar cell.

As can be seen from Fig. S7, the maximum power density of the tandem solar cell is found to be $5\mathrm{mW/cm^2}$ for a $(1+Z)$-value of 1.054. However, the power density stays constant within the error margin between $(1+Z)$-values of 0.99 and 1.07. Because the effective irradiance during spectrometric characterization was $100\mathrm{mW/cm^2}$ the efficiency for the AM1.5g spectrum, defined as $(1+Z)=1$ here, is 5%. In contrast, j_{sc} of the tandem solar cell shows a maximum for a $(1+Z)$-value of 1.15 which corresponds to a much more blueish spectrum. The reason for the different positions of these maxima is the behavior of the fill factor. FF continuously decreases for increasing $(1+Z)$ until a value of 1.18 and stays constant for higher values. This behavior can be explained by a strong difference of the fill factors of the subcells. The subcell with the higher fill factor (in this case the green absorbing subcell) determines the fill factor of the tandem solar cell as long as it is very clearly the current limiting one. If the JV-characteristics of the subcell with the lower fill factor (in this case the red absorbing subcell) is now shifted to lower currents, i.e. the illumination intensity on this subcell is decreased, the fill factor of the tandem cell begins to decrease exactly when the crossing point of both subcell JV-characteristics reach the MPP of the subcell with the higher fill factor. Then the fill factor of the tandem cell decreases until it

DOI: 10.1038/NPHOTON.2015.124

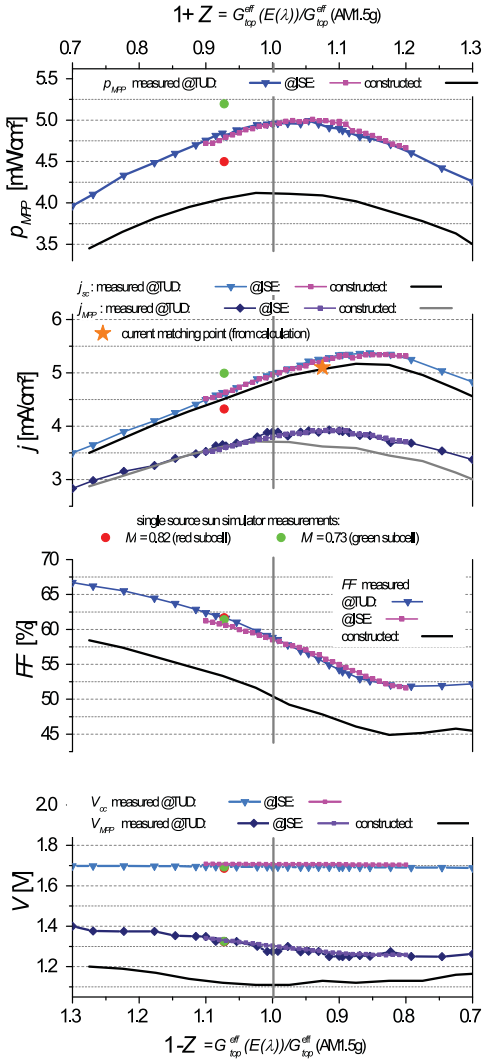

Fig. S7: *Spectrometric characterization results for tandem organic solar cell sample A measured at TUD and ISE. The values of ISE are scaled using another effective solar cell area for calculating current densities for reasons of comparability. The characteristic values achieved with a single-source sun simulator at TUD calibrated in respect to the mismatch factors of the green absorbing subcell as well as the red absorbing subcell are shown for comparison. The curves denoted as constructed as well as the current matching point are calculated from JV-curves of the subcells constructed from EQE results measured at TUD as described in subsection 3.3.*

has reached the value of the fill factor of the subcell with the lower fill factor and stays constant. Since non-ideal fill factors are often found for organic solar cells, this behavior can be considered as typical.

In Fig. S7, the characteristic values of the JV-characteristics achieved with a single-source sun simulator, calibrated in respect to the mismatch factors of the subcells already shown in Fig. S5, are plotted for comparison at $(1 + Z) = 0.93$. This value corresponds to the spectrum of the used single-source sun simulator being calculated from equation 6 by assuming $A_2 = 0$. Applying the mismatch factor of the red absorbing subcell, power density as well as current density are reduced compared to the spectrometric characterization. In contrast, applying the mismatch factor of the green absorbing subcell, power density as well as current density are overestimated by 8 %. FF and voltage do not change compared to spectrometric characterization regardless the applied mismatch factor.

The reason for this behavior is the differing effective irradiance for both methods. As shown in section 2, the effective irradiance on the tandem solar cell during the spectrometric characterization is always that of the reference spectrum, which is 100mW/cm^2 in the shown experiments. Since for $(1 + Z) = 0.93$ the spectrum is red shifted compared to SRC at $Z = 0$, the effective charge generation in the green absorbing subcell is reduced. This also reduces the current of the tandem solar cell since this subcell is current limiting. On the contrary, for the measurement under the single source sun simulator the current generation of the green absorbing subcell is increased to that at 100mW/cm^2 by using the respective mismatch factor M. Therefore, the measured j_{sc} under the single source sun simulator is significantly higher than the respective value on the 'line of measurement' (for $(1 + Z) = 0.93$) and equals exactly the SRC-value. In contrast, the fill factor and the voltages almost perfectly coincide with the values on the 'line of measurement' because they do not depend on the irradiance in the relevant range of intensity variation. These findings explain the overestimation of the efficiency: While the j_{sc} equals the SRC-value due to the increased irradiance resulting from spectral mismatch correction, the fill factor is measured for a wrong spectrum. Since for this spectrum the fill factor of the subcells with the higher fill factor dominates, it is considerably overestimated. Consequently, the multiplication of j_{sc}, FF, and V_{oc} leads to an overestimated efficiency.

Even though, the used single-source sun simulator is a class AAA sun simulator its spectral deviations compared to AM1.5g lead to a significant impact on the characteristic values. The findings also show, that single-source sun simulators are principally inappropriate for the characterization of tandem organic solar cells and will generally lead to wrong results. Only if the mismatch factors of both subcells in respect to the used single-source sun simulator are coincidentally equal, the results would be correct.

According to reference[87] the maximum j_{sc} value in the spectrometric characterization can be identified with the so-called current matching point where the short circuit currents of both subcells are equal. The knowledge of the current matching point reduces the degree of freedom in the system of linear equations (equ. 6 and 7), leading to a spectral characterization allowing the calculation of the scaling factors c_{top} and c_{bot} resulting in the absolute spectral responses

$$S_{top}(\lambda) = c_{top} s_{top}(\lambda) \tag{11}$$

and

$$S_{bot}(\lambda) = c_{bot} s_{bot}(\lambda)\,, \tag{12}$$

respectively. This way, it is possible to determine the absolute spectral response, even though only relative spectral response data was used for spectral metric determination.

However, for tandem solar cells consisting of subcells with strongly differing fill factors, the maximum j_{sc} value in the spectral metric and the current matching point can differ significantly. This case is not considered in reference[87] since it is hardly relevant for inorganic tandem solar cells. Therefore, in the following section an alternative procedure to determine absolute spectral responses of the subcells of a tandem solar cell is presented.

DOI: 10.1038/NPHOTON.2015.124

3.3 Subcell Characterization

The main reason for the complicated measurement procedure of tandem solar cells is the inaccessibility of the individual subcells. The characterization process of tandem solar cells could be much easier if there were access to the subcells' spectral response, JV-characteristics, or at least their voltage during tandem cell JV-characterization. Furthermore, some of the challenges described in section 2 of the main text would be trivial if the subcells could be characterized separately, especially the determination of the necessary bias voltage for SR-measurements of tandem solar cells. However, electrical access to the recombination contact between both subcells is necessary to realize such measurements. There are three approaches to achieve this: First, it is possible to obtain information about the subcells without any changes on the solar cell stack by using SR-measurements under specific bias illumination and bias voltage.[90] Hereafter, this approach is called "Bias-Voltage Approach". Second, inserting an intermediate conductive interlayer in the recombination contact. This way it is possible to extract current (and voltage) from both subcells separately. Hereafter, this approach is called "Current Contact Approach". Third, an electrode contacting the recombination layer but being situated outside the active area of the solar cell can be used.[90] By this means, it is not possible to extract current from the subcells since the lateral conductivity of the recombination contact itself is in general not sufficient, but the voltage of both subcells can be measured. Hereafter, this approach is called "Voltage Contact Approach".

All three approaches are presented in the following, while focusing on the Bias-Voltage Approach, since it can be applied to existing samples without necessity to process new devices. It is directly applied to tandem solar cell stack A (see Fig. S3) and the results are related to the spectrometric characterization.

Bias-Voltage Approach

With the first method, electrical characterization of the subcells is possible by exploiting the spectral response measurement of the tandem solar cell in a two-terminal device. Varying the bias voltage across the tandem cell enables the determination of a JV-curve of the subcell under appropriate bias illumination. Fig. S8(a) and (b) show EQE spectra of device A under varying bias voltage and bias illumination. According to section 3.1 the exact determination of the EQE of the subcell requires a specific illumination and an electric forward voltage. Measuring the EQE of the subcells at variable bias voltages and calculating j_{sc} of the subcells by integrating the product of EQE and AM1.5g solar spectrum over λ corresponds to measuring the JV characteristics of the subcells. However, in an EQE-measurement only the photocurrent being the response of the cell to modulated light is measured but no injected non-modulated current. Consequently, the constructed JV characteristics is actually the $J_{photo}V$ characteristics. We note that the relation $j_{photo} = j_{light} - j_{dark}$ is valid below V_{oc}[102] meaning that the JV characteristics below V_{oc} can be calculated if the $J_{dark}V$ characteristics is known. The leveling off of the photocurrent near and above V_{oc} that can also be observed for device A (see Fig. S8(c)) originates from the effective voltage over the solar cells being much less than the applied voltage because of a non-negligible series resistance in the electrodes. A reduced forward photocurrent is expected when photogenerated carriers can effectively recombine with injected charges. This regime is however less relevant for the characterization of the subcells. After integrating the product of the EQE and the AM1.5g solar spectrum for variable electrical bias, the current densities of front and back cell can be plotted vs. the bias voltage on the tandem cell. To these curves the respective forward bias voltage on the tandem solar cell is added, shifting the curves. By this means the correct short-circuit current densities are displayed at 0V. Subcell JV-characteristics of device A determined according to this procedure are shown in Fig. S8(c). Due to the recombination of photogenerated and injected charge carriers, the slope of the JV-curve towards V_{oc} decreases significantly such that the constructed $J_{photo}V$-curves does not cross the x-axis towards positive currents.

The JV-curves of the subcells are series connected and according to Kirchhoff's law, their voltage at equal current densities can therefore be summed to result in the $J_{photo}V$-curve of the tandem cell. In a second step, the addition of the photocurrents of this $J_{photo}V$-curve to the separately measured $J_{dark}V$-curve of the tandem cell will lead to the JV-curve of the tandem cell under illumination. The JV-curve of tandem solar cell device A achieved with this method

is shown in Fig. S8(c) as well as the one measured with the JV-measurement setup at TUD for comparison. The measured and the calculated curve show an excellent agreement up to 0.9V. Above 0.9V the reduced slope of the calculated subcell JV-curves affects the constructed tandem JV-curve leading to a reduced slope compared to the measured curve. For positive currents both curves perfectly match again since the added dark characteristics dominate.

If the device shows a nonlinear intensity dependence, this procedure can significantly depend on the bias light intensity which will lead to deviations of the calculated JV-curve as well as the calculated short-circuit current densities from real values. Therefore, this method should be used carefully and a comparison with one of the other approaches is recommended.

However, the knowledge of the JV-curves of the subcells in conjunction with spectrometric characterization makes a method available allowing the determination of the calibration factors c_{bot} and c_{top} for calculating absolute spectral responses (see eq. 11 and 12), as described in the following.

If one assumes that the fill factors of the subcells are independent on the irradiance, which can in fact be assumed for the irradiance variations relevant here, the constructed JV-curves of the subcells can be used to calculate the tandem solar cell characteristics for any illumination spectrum and any irradiance meaning for any point $(G_{eff}^{top}, G_{eff}^{bot})$ of the spectral metric of the respective tandem solar cell. The spectral metrics of tandem solar stack A resulting from this calculation are shown in Fig. S7. Restricting this calculation to a subspace where the condition $j_{sc}^{bot} = j_{sc}^{top}$ is fulfilled results in all possible 'lines of measurement'. The selection of the 'line of measurement' corresponding to the experiment is done by fitting the calculated tandem solar cell j_{sc} to the measured curve. The resulting c_{top} and c_{bot} allow the calibration of the constructed subcell JV-characteristics, and therefore the calculation of the absolute spectral response.

The application of this procedure to tandem solar cell stack A results in the constructed spectrometric characterization shown in Fig. S7. The behavior of the j_{sc} can be reconstructed very well, whereas calculated V_{MPP}, and therefore also p_{MPP} and FF are significantly lower than the measured values. However, their qualitative behavior can be reconstructed. Reason for the quantitative deviations is the constructed $J_{photo}V$-curve in contrast to the real $J_{photo}V$-curve does not cross the x-axis towards positive currents and therefore shows a reduced slope for voltages above 0.9V.

Current matching is identified for a $(1-Z)$-value of 0.925 where the calibrated current of the tandem solar cell is 5.1mA/cm^2. Dividing this current value by $(1+Z)$ and $(1-Z)$, the j_{sc} under AM1.5g for the top and the bottom subcell are determined to be 4.7mA/cm^2 and 5.5mA/cm^2, respectively. Comparing these values to the j_{sc} calculated from the EQE-spectra (cp. Table S2) shows that the spectra measured by Fraunhofer-ISE exhibit the smallest deviation with a correction factor $c_{bot} = 0.95$ and $c_{top} = 1$. This means the measured EQE-spectrum for the top cell is identical to the absolute EQE-spectrum.

As mentioned before, knowing the JV-characteristics of the subcells allows to calculate the spectral metric for any illumination spectrum, e.g. the spectrum at sunrise or sunset. The spectral matrices of p_{MPP}, j_{sc}, FF, and V_{MPP} for tandem solar cell stack A are shown in Fig. S9. The quantity $(1+Z)$ on the x-axis corresponds to the effective irradiance on the top cell (green absorbing subcell) under the spectrum $E(\lambda)$ normalized by the effective irradiance under the reference spectrum AM1.5g $G_{eff}^{top}(E(\lambda))/G_{eff}^{top}(\mathrm{AM1.5g})$. Analogously, $(1-Z)$ corresponds to the effective irradiance on the bottom cell (red absorbing subcell) under the spectrum $E(\lambda)$ normalized by the effective irradiance under the reference spectrum AM1.5g $G_{eff}^{bot}(E(\lambda))/G_{eff}^{bot}(\mathrm{AM1.5g})$. Therefore, the units on the scales in Fig. S9 indicate the effective irradiance in 'suns'. In each spectral metric the 'line of measurement' as well as the AM1.5g spectrum are shown. Since the 'line of measurement' is defined for an irradiance of 100mW/cm^2, the crossing point of both lines has the coordinate (1,1) corresponding to SRC. There, both subcells receive the exact effective irradiance of the standard spectrum AM1.5g. Further details on the spectral metric concept can be found in reference[87].

In Fig. S9 the spectrum of the single source sun simulator used for the measurements according to the mismatch factors of the subcells (cp. Fig. S7) is represented as dotted line and the two irradiances according to the mismatch factors of the subcells are depicted as stars to illustrate the deviation compared to a measurement under SRC. The filled star represents the measurement

DOI: 10.1038/NPHOTON.2015.124

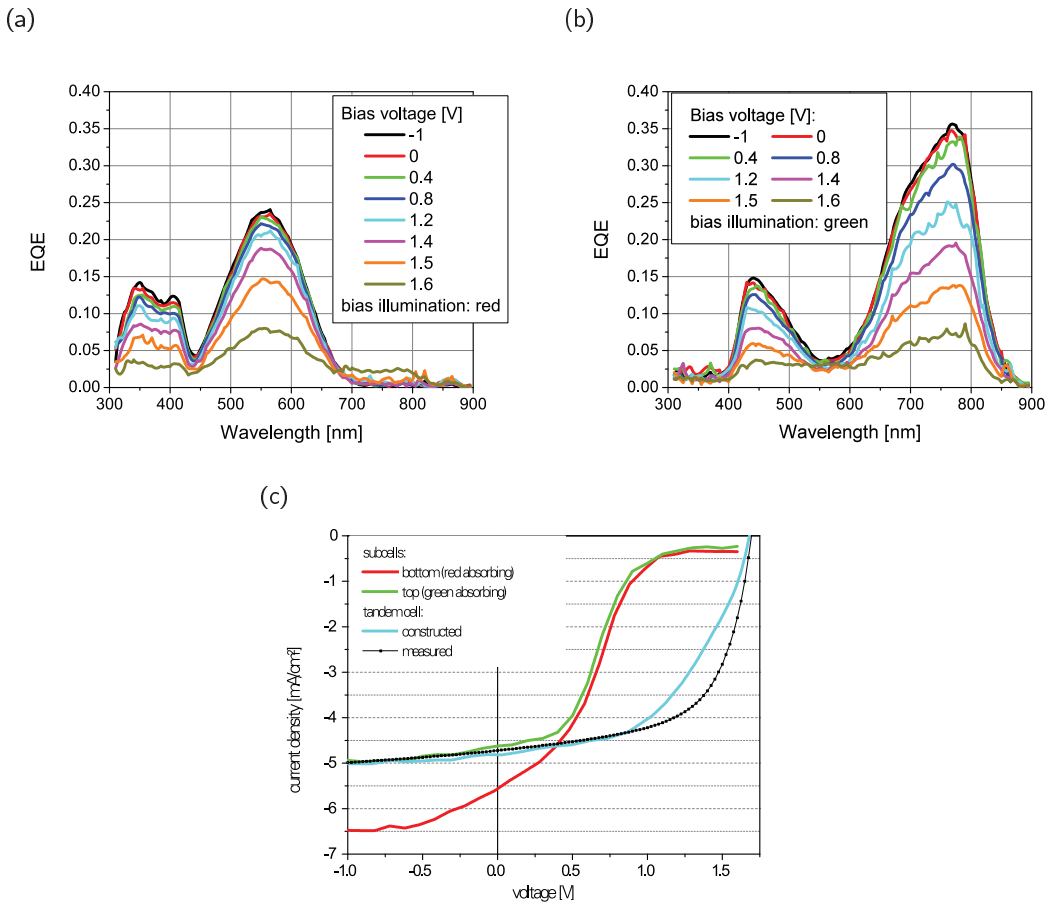

Fig. S8: *(a) EQE spectra of the bottom cell of tandem solar cell sample A for selected bias voltages (measured under green bias illumination) and (b) those of the top cell (measured under red bias illumination). (c) $J_{photo}V$-characteristics of the subcells calculated from the EQE spectra as well as the tandem solar cell characteristics calculated thereof with the $J_{dark}V$-characteristics added to be comparable to the measured JV-curve that is also shown. To assure comparability all characteristics are shown for Z=0 meaning for SRC.*

with the top cell being mismatch corrected. Therefore it is located at a $(1 + Z)$-value of 1. In contrast, the open star represents the measurement with the bottom cell being mismatch corrected and is therefore located at a $(1 - Z)$-value of 1. However, due to the sun simulator spectrum deviating from AM1.5g, both stars are quite far away from the coordinate (1,1) in the spectral metric corresponding to SRC.

Furthermore, the depiction of the characteristic values of the tandem solar cell in Fig. S9 allows conclusions about the behavior of the solar cell for spectra that have not been directly accessed by spectrometric characterization. Consequently, it can be used for optimization or for long term output forecasts under varying spectra.

Current Contact Approach

The current contact can be realized for example by inserting thin metal interlayers that have been demonstrated to work as electrodes for semitransparent small-molecule as well as polymer-based organic solar cells[21,103–106]. The actual material does not matter, the main requirement is that interlayers relevant here must have lateral conductivities sufficiently high to extract the photocurrent of the solar cell without significant losses. Layers of metal clusters embedded into organics, as introduced for recombination layers in organic tandem solar cells[107,108] for example, do not fulfill this requirement.

In tandem solar cell sample B1 (see Fig. S10(a) for layer stack), metal interlayers are introduced to demonstrate its function as intermediate contact for the characterization of the subcells. The exact composition of the metal interlayer is optimized according to reference[103]. In Fig. S11(a) the JV-characteristics of sample B1 and its subcells are shown. Furthermore, from the subcell JV-characteristics, the tandem solar cell JV-characteristics are constructed and show a perfect coincidence with the measured one. In Fig. S11(b) the EQE spectra of sample B1 are depicted. For each subcell two measurements have been performed: Firstly, contacting the entire tandem solar cell and using conventional bias illumination in conjunction with lock-in technique, and secondly, contacting the subcells directly without using any bias light. The curves show slight deviations in absolute values that can be attributed to the discussed nonlinearities of the photocurrent. However, normalizing the spectra (not shown) results in a very good coincidence.

Hence, the current-contact approach allows full access to the subcells of an organic tandem solar cell, and therefore, in conjunction with spectrometric characterization, enables an exact measurement under SRC and the calculation of the complete spectral metric. The spectrometric characterization procedure is much simplified as the effective irradiances of the subcells can directly be measured as the ratio of the mismatch corrected j_{sc} of the subcells.

However, inserted metal layers interfere with the optical electric field inside the device, as well as contribute to parasitic absorption, leading to results not comparable to the original tandem solar cell without intermediate metal contact. Therefore, this approach should mainly be used for fundamental studies, but the results should not be transfered to solar cells without current contact unless the current contact can be made really transparent.

Voltage Contact Approach

In contrast, the Voltage Contact Approach has the advantage that there is only very little influence on the absorption in the active absorbing area of the solar cell stack since the contact is placed outside the active area. The contact has to be placed as near as possible to the recombination contact. However, due to the low lateral conductivity of the used materials, a current can generally not be extracted, but the voltage drop over both subcells can be measured.

Figure S12 shows the JV-characteristics of tandem solar cell stack B2 (see Fig. S10(b) for layer stack), and its subcells. The current density is measured at the tandem solar cell, which is identical to the subcell current density due to series connection, while the voltages of the subcells are measured individually. From the subcell JV-characteristics, the tandem solar cell JV-characteristics are constructed and show a perfect coincidence with the measured ones. The voltage-contact approach is therefore a practically feasible method to determine the subcells' JV-characteristics with high accuracy and at exactly the tandem solar cell structure to be measured. A drawback of this

DOI: 10.1038/NPHOTON.2015.124

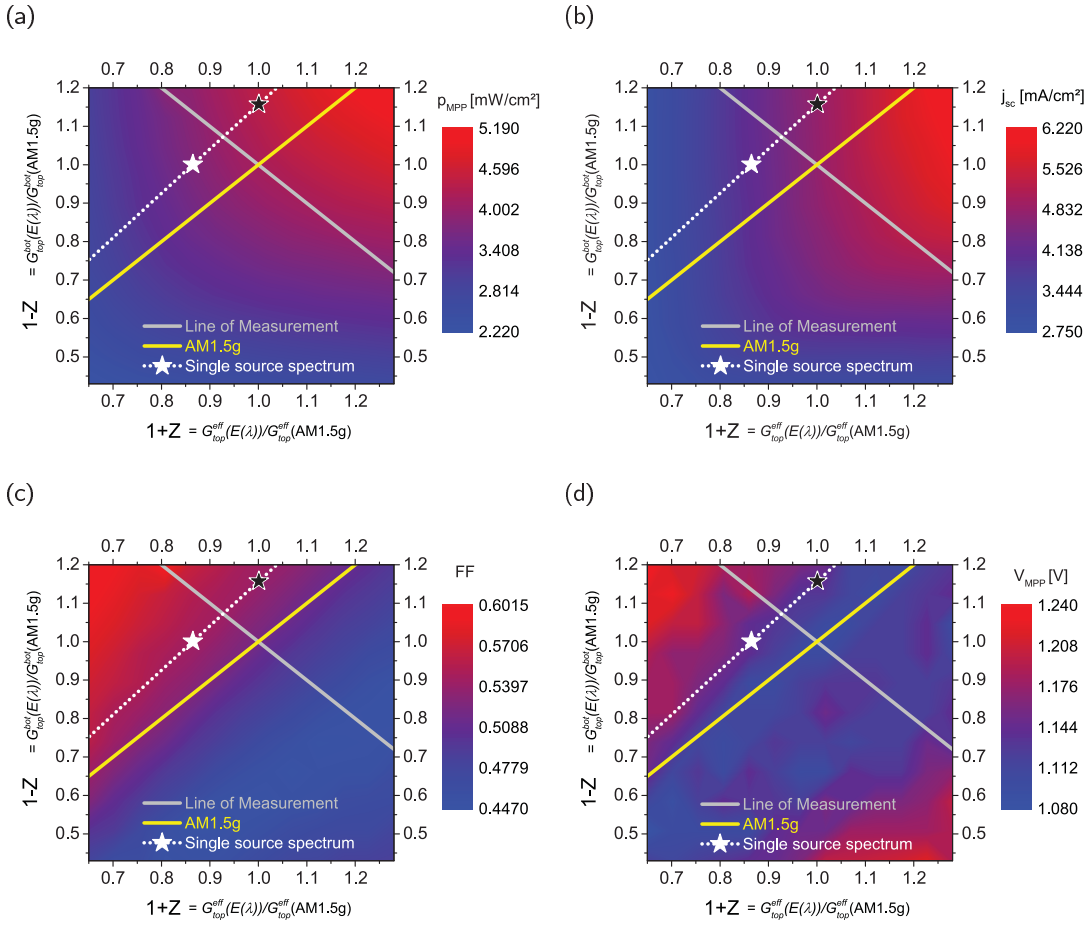

Fig. S9: *Full spectral metrics of tandem solar cell sample A calculated from the subcell JV-characteristics shown in Fig. S8 for (a) Maximum power density p_{MPP}, (b) short circuit current density j_{sc}, (c) Fill factor FF and (d) voltage at maximum power point (MPP) V_{MPP}. The calibration to AM1.5g is based on the fitting to the line of measurement. The dotted line represents the spectrum of the single source sun simulator at different irradiances. The irradiances corresponding to the mismatch factors of the top cell and the bottom cell are marked with a filled and an open symbol, respectively.*

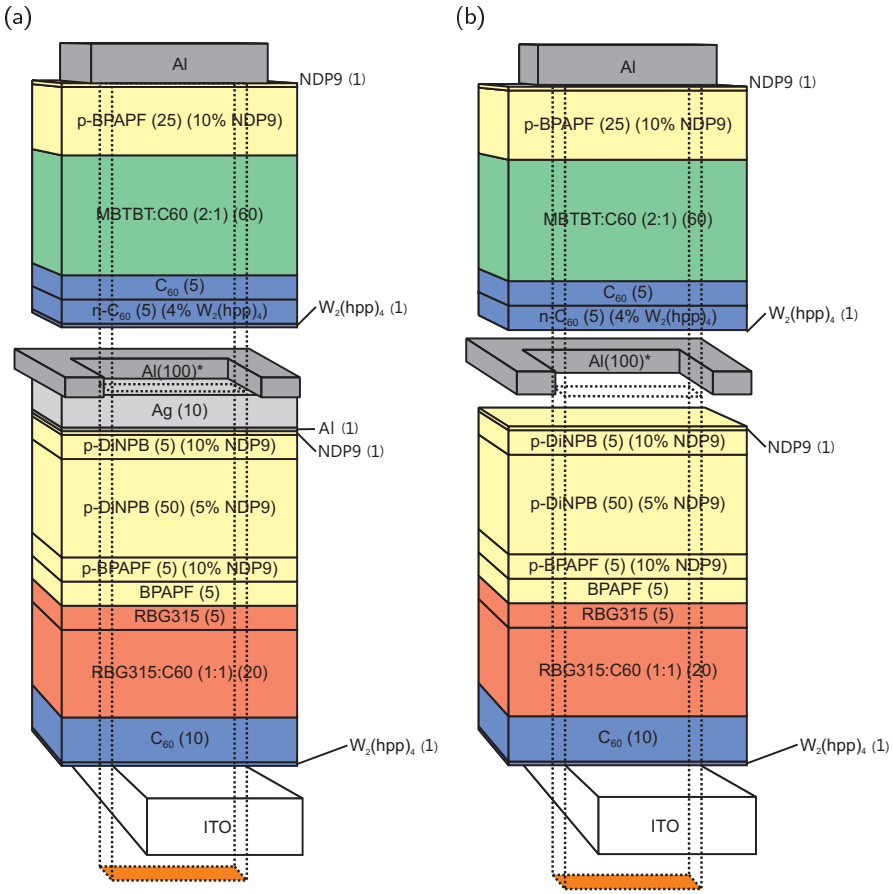

Fig. S10: *Layer stack of (a) tandem solar cell sample B1 and (b) sample B2 with thicknesses given in nm. For the evaporation of the starred Al-layer a shadow mask has been used such that the layer itself is situated around the active area having only little influence on the tandem solar cell. The overlap of the ITO, the organic layers and the metal contact that is indicated by the dotted lines is used as the active area of the solar cell, the size of which is suggested by the orange area. Thus, with sample B1 comprising a recombination contact consisting of a laterally conductive Ag-layer a 'current contact' is achieved while with sample B2 a 'voltage contact' is realized.*

DOI: 10.1038/NPHOTON.2015.124

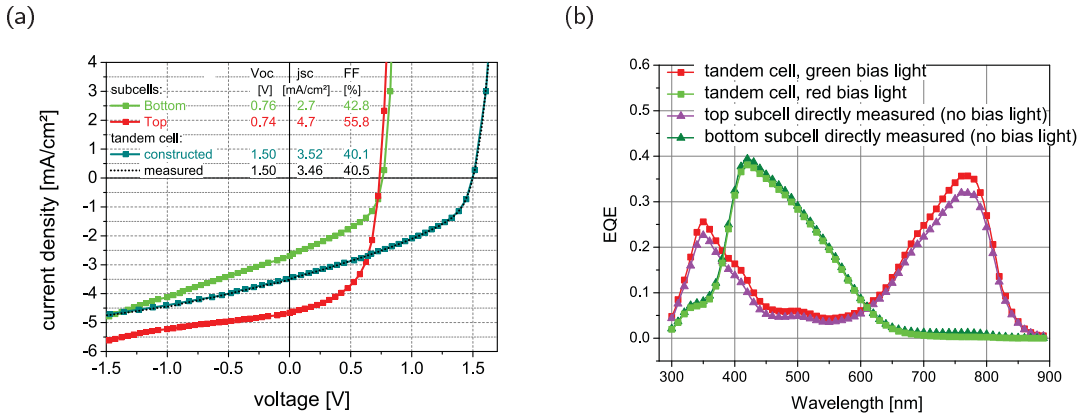

Fig. S11: *JV-characteristics measured using the Current Contact Approach. (a) JV-characteristics of the subcells of tandem solar cell sample B1 as well as the constructed and measured tandem solar cell JV-curves that coincide very well . (b) EQE of the subcells of sample B1 measured conventionally with bias illumination and by using the current contact without using any bias illumination showing only slight relative deviations.*

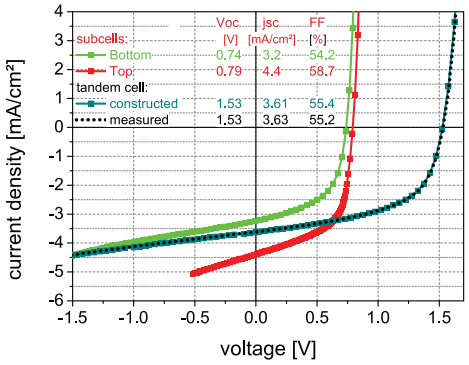

Fig. S12: *JV-characteristics of the subcells of tandem solar cell sample B2 using Voltage Contact Approach. The voltage during subcell characterization was measured via the intermediate voltage contact. The tandem solar cell JV-curve constructed from the subcell's JV-characteristics and the directly measured tandem solar cell JV-curve is also shown.*

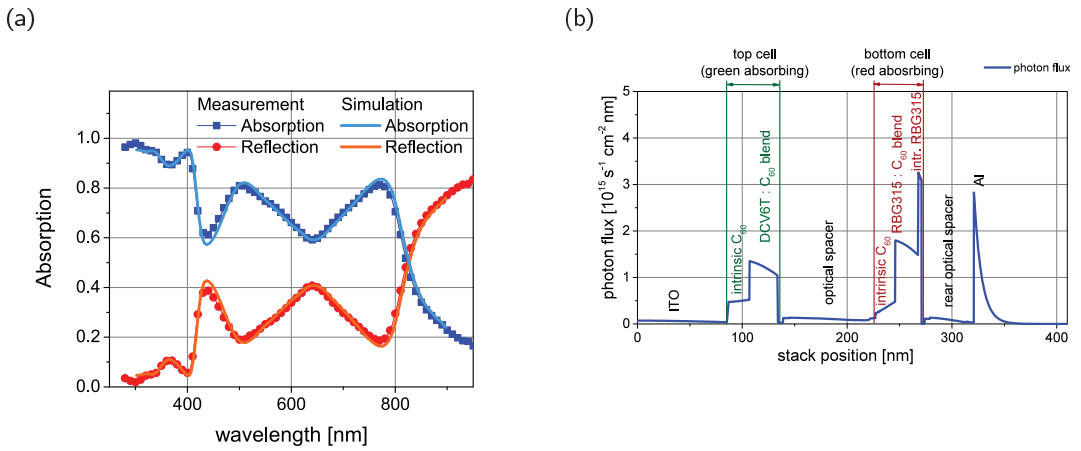

Fig. S13: *(a) Absorption measured in reflection and simulated absorption and (b) absorption profile of solar cell stack A. In (b) the organic layers contributing to the photocurrent are identified for each subcell.*

approach is the necessity of very carefully designed and accurately processed electrodes. In contrast to the Current Contact Approach, the spectrometric characterization has to be conducted as described in subsection 3.2, since there is no access to the currents of the individual subcells.

3.4 Optical Simulation and *IQE*

The calculation of the absorption of tandem solar cell stacks using optical parameters of the incorporated materials as well as the stack configuration allows optimizing devices but also provides important information for characterization. First, the decision for the bias light spectra for spectral response measurements can be based on the calculated absorption within the active layers of the subcells. Due to interference effects in the solar cell stack, the absorption of certain layers in the stack significantly differs from those measured on single layers that therefore should not be the only basis of the decision for a particular bias light. Second, it is possible to validate spectral response measurements of the subcells by comparing them to the simulated absorption of the subcells.

The first step of the procedure is an optical simulation of the stack. By fitting the results of the simulation to the measured absorption spectrum of the solar cell stack, a correction of the layer thickness values, being the basis for the simulation, is possible. With the corrected simulation, the absorbance of each single layer of the solar cell, especially of the absorber layers contributing to the photocurrent, can be calculated. Dividing the *EQE* by the calculated absorption of the active layers contributing to the photocurrent gives an effective internal quantum efficiency IQE_{act} [109]. This way, *IQE* values are independent of parasitic absorption and only reflect the electrical behavior of the solar cell. Moreover, this calculation is possible for each subcell individually, which allows a qualitative validation of the *EQE* results. *IQE* exceeding 1 or absorption spectra strongly deviating from the shape of the *EQE* spectra are hints for errors, e.g. that the wrong subcell has been addressed during *EQE*-measurement.

In the following the described procedure is applied to solar cell stack A. Figure S13(a) shows the absorption measured in reflection as well as the optimized simulated absorption for the investigated solar cell stack. The root-mean-square deviation between measured and calculated data is below 2%. With the fitted simulation data, the absorption in each single organic layer is calculated. One result of this calculation is the photon flux profile in the solar cell, being depicted in Fig. S13(b). The intrinsic and blend layers considered as contributing to the photocurrent of the subcells are marked - hereafter these layers are called active layers.

The sum of the absorption of the active layers is shown for the green and the red absorbing subcell in Fig. S14(a) and (b), respectively. The *IQE* calculated from the active layer absorption

DOI: 10.1038/NPHOTON.2015.124

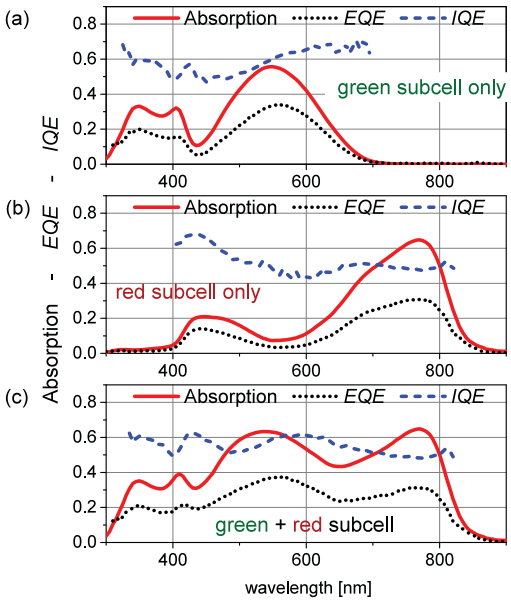

Fig. S14: *Simulated absorption, absolute EQE, and internal quantum efficiency IQE for (a) the green and (b) the red absorbing subcell as well as (c) the sum of both subcells, respectively. The simulated absorption only takes those organic layers into account that contribute to the photocurrent. The shown internal quantum efficiency calculated from this absorption data is therefore not influenced by parasitic absorption and only reflects the electrical behavior of the solar cell.*

and the absolute EQE as determined in section 3.3 is depicted as well. The IQE for the green subcell varies from 50% to 70% and does not show an unexpected behavior[95], being a strong hint that the shown EQE spectra in fact belong to the intended subcells meaning bias light conditions have been set properly. The same applies to the red subcell. In Fig. S14(c) absorption, EQE as well as IQE of the red and the green absorbing subcell are added. One can see that the solar cell presented has an average effective internal quantum efficiency of 55%.

4 General rules for characterizing tandem organic solar cells

Finally, in this section the full guidance for characterizing tandem organic solar cells including further additional optional steps that can improve validity and accuracy, but are not considered to be mandatory.

1. Estimate the bias light conditions for the SR-measurement. Select the spectrum of the bias light according to the absorption spectrum of the absorber materials. If both subcells comprise identical absorber materials, proceed as given in reference[89]. Select the intensity of the bias light such that always the intended subcell is being measured.

   Option 1 a): Determine the intensities of the bias light by detailed optical simulation, ensuring the subcell to be measured exhibiting the lower charge generation but provide at least some flood light.

   Option 1 b): If it is possible to process tandem solar cells with an intermediate contact according to the Current Contact Approach having exactly the same structure as the test cell, use them to check the linearity of the SR depending on bias light intensity.

2. Estimate the bias voltage conditions for the SR-measurement based on the expected voltages of the subcells. As a first approximation, the open circuit voltages V_{oc} of single solar cells incorporating the same absorber system can be used.

   Option 2 a): If for any reason the exact determination of the bias voltage is not possible, the EQE spectrum has to be measured dependent on the bias voltage. If the normalized EQE spectra coincide, i.e. bias-voltage being independent on the relative EQE, any bias voltage can be used for the further procedure.

   Option 2 b): If single junction dummy cells comparable to the subcells of the tandem cell are available, a detailed analysis for determining the bias voltage according to reference [88] should be carried out.

   Option 3 c): The highest accuracy for bias voltage determination can be achieved by realizing subcell characterization with a voltage contact according to subsection 3.3. It should be noted that beyond that, with subcell characterization a complete spectral response or even JV-measurement on each separate subcell is possible.

3. Measure the SR of both subcells according to standard ASTM E2236 using chopped monochromatic light in conjunction with lock-in technique applying the above determined bias voltage and bias light conditions. Additionally, measure the SR without bias light and check if it follows the lower envelope of the spectra with bias light.

4. Based on the results of the SR-measurement, determine the intensities of the two sources of a spectrally adjustable sun simulator such that both subcells of the test tandem solar cell are mismatch corrected. Use either the iterative procedure of standard ASTM E2236 or the methods described in references[87,110]. Measure the JV-characteristics of the solar cell and determine the efficiency. Since the effective solar cell area has a crucial influence on the efficiency, put emphasis on its determination according to references[97–101]. The aperture size should be the same as used for SR-measurement.

DOI: 10.1038/NPHOTON.2015.124

Option 4 a): Do a spectrometric characterization and consequently identify the current matching point of the tandem cell. Calculate the absolute SR. If the fill factors of the subcells differ significantly use the procedure described in subsection 3.3 of this paper.

Option 4 b): Conduct an absorption measurement of the test solar cell and, in conjunction with optical simulation, calculate the absorption in each of its layers. The calculation of the IQE and its comparison to EQE allows a validation of the SR-measurement.

The most frequent deviation compared with the recommended standard procedure is a missing spectrally adjustable sun simulator. For tandem solar cell sample A, the efficiency is overestimated by 4% (relative) using a single- instead of a multi-source sun simulator. However, depending on the exact device behavior and on the sun simulator spectrum, the deviations can be much higher.

It should be noted, that the given procedure is not sufficient for achieving correct results for semitransparent organic solar cells, as back reflections from the measurement chuck contribute to the effective irradiances. These reflections are spectrally selective and will influence the spectral sensitive performance of multi-junction devices. Thus, for ensuring standard irradiance, possible reflections need to be taken into account. Generally, the back reflection conditions should be similar to the application conditions of the solar cells. To ensure comparability, the exact back reflection conditions should be stated if such results are published.

5 Synopsis

An analysis of publications from the field of tandem OPV shows that only in 4% of the 73 papers reviewed in this work, efficiency values of tandem organic solar cells were measured according to the relevant standards. This malpractice is attributed to a missing awareness of the standards and/or the use of inadequate experimental infrastructure. Furthermore, certain peculiarities of organic solar cells compared to inorganic ones, for which the standards were originally developed, necessitate special care when applying the standards to tandem OPV.

The relevant standards, especially ASTM E2236[3] and the equally valid procedure suggested by Meusel et al.[87], are reviewed and applied to a tandem organic solar cell with complementary absorbers. Therefore, the following characterization steps are carried out: First, the spectral response is measured by three independent institutes. Second, the JV-characteristics under a class AAA sun simulator applying the mismatch factor of the current limiting subcell for calibration is measured and the corresponding efficiency is calculated. Third, a correctly AM1.5g-calibrated JV-measurement using a spectrally adjustable sun simulator is done and the corresponding efficiency is calculated. Fourth, an additional full spectrometric characterization is carried out by two independent institutes. Fifth, the "Bias Voltage Approach for subcell characterization" is introduced to calculate the complete spectral metric from the JV-characteristics of the subcells that are derived from EQE-measurements under varying bias voltage according to reference[90]. Sixth, absorption measurements and detailed optical simulations are carried out. Finally, in addition to the "Bias Voltage Approach" the "Current Contact Approach" and the "Voltage Contact Approach" are presented by means of the characterization of corresponding tandem solar cell stacks to show their adequacy for the direct characterization of the subcells of tandem organic solar cells.

The relative EQE-spectra measured by the three independent institutes according to ASTM E2236[3] show only slight deviations suggesting the used measurement procedures are appropriate for gaining standard-compliant results. Nevertheless, absolute SR being not mandatory for correct characterization deviates by up to 20%.

The JV-characterization using a single source sun simulator resulted in an efficiency of 5.2% whereas for a correctly calibrated measurement using a spectrally adjustable multi-source sun simulator it is 5.0%. The spectrometric characterization results that show exactly the same spectral dependence for both measuring institutes except for the solar cell area calibration, fully explains this efficiency deviation. The reasons are differing fill factors of the subcells of the measured tandem solar cell in conjunction with differing mismatch factors of the subcells in respect to the used sun simulator. Therefore, the fill factor of the current limiting subcell is overestimated compared to

the calibrated measurement, while the current density equals that one at SRC. Consequently, the efficiency is overestimated. The results show that the efficiency determination using a single-source sun simulator will generally be misleading except the mismatch factors of both subcells in respect to the used sun-simulator are coincidentally identical which, however, is very unlikely.

The application of the "Bias Voltage Approach for subcell characterization" allows the identification of the current matching point and according to reference[87] the calculation of the absolute spectral response. The deviation between measured relative EQE and absolute EQE is found to be below 5%, at least for the measurement of Fraunhofer-ISE.

It is shown that optical simulations in conjunction with absorption measurements on the tandem solar cell stack can be used for validating the measured EQE-spectra and to calculate the IQE of the subcells separately.

The "Voltage Contact Approach" and the "Current Contact Approach" turned out to be adequate intermediate contact techniques to determine the JV-characteristics of the subcells directly and thereof the correct SR-measurement conditions of the the tandem solar cell such as bias voltage and bias light.

In conclusion, we present practical rules for the characterization of tandem organic solar cells that should be established as a standard in the OPV community. The most important issue of these rules is the inappropriateness of single-source sun simulators for tandem solar cell characterization. Publications stating record efficiencies of tandem organic solar cells should never be accepted if the measurement is not based on a spectrally adjustable sun simulator. For non-record values at least the spectral mismatch of the subcells should be discussed in detail and the exact experimental infrastructure should to be described. This way, reliability concerning the published results can be established, being essential for the future economic success of organic photovoltaics or other emerging solar cell technologies.

6 Experimental

Before use, all organic materials were purified by vacuum gradient sublimation, except the n-dopant and the p-dopant that were used as received. C_{60} (Fraunhofer Institut Photonische Mikrosysteme (IPMS) Dresden, Germany) (LUMO: -4.0eV) was used as electron transport material and as acceptor in blend layers with the absorber materials. As n-dopant tetrakis(1,3,4,6,7,8-hexahydro-2H-pyrimido[1,2-a]pyrimidinato)ditungsten (II) and as p-dopant NDP9 (both Novaled AG, Dresden, Germany) was chosen. As absorber materials α,ω-bis-(dicyanovinylen)-sexithiophene (DCV2-6T-Bu(1,2,5,6)) (Heliatek GmbH, Dresden, Germany) and aza-Boby-H[111] (Synthesized in TU Dresden labs) as well as 4,7-bis(5'-methyl-2,2'-bithiophen-5-yl)benzo[c][1,2,5]thiadiazole (MBTBT)[112] (supplied by Bergische Universität Wuppertal, Wuppertal, Germany) were used as donors in blend layers with C_{60}. N,N-diphenyl-N,N-bis4-N,N-bisnaphth-1-yl-amino- biphenyl-4-yl-benzidine Di-NPD (Sensient) and 9,9-bis4-N,N-bis-biphenyl-4-yl-aminophenyl-9H-fluorene BPAPF (Lumtec) served as hole transport layers. All devices were prepared on indium tin oxide - coated glass substrates (Thin Film Devices Inc., Anaheim, USA) with a sheet resistance of 30Ω/□ precleaned with organic solvents in an ultrasonic bath. Thermal evaporation was performed at p<10-7 mbar and deposition rates of ~ 0.5 Å/s in an UHV-chamber (Kurt J. LESKER Co. Ltd., Hastings, UK) .

Doping was realized by coevaporation of matrix and dopant material from different crucibles while the deposition rates are individually controlled by quartz oscillators. The resulting solar cell devices had an area of 6.44mm^2 that is defined by the overlap of the active layers, the aluminum and the ITO.

After processing, all devices were transferred from vacuum directly into an inert gas atmosphere and were encapsulated there with epoxy sealed glass covers. The encapsulated samples were characterized in air.

For the determination of the differential spectral response at TUD, a custom-made setup was used. The monochromatic beam (Oriel Xe Arc-Lamp Apex Illuminator combined with Cornerstone 260 1/4m monochromator, both Newport, USA) probing the device was mechanically chopped at a frequency of 211Hz and the corresponding current response of the device was measured via a lock-in amplifier 7265 DSP (Signal Recovery, UK). This allows for additional constant bias illumination

DOI: 10.1038/NPHOTON.2015.124

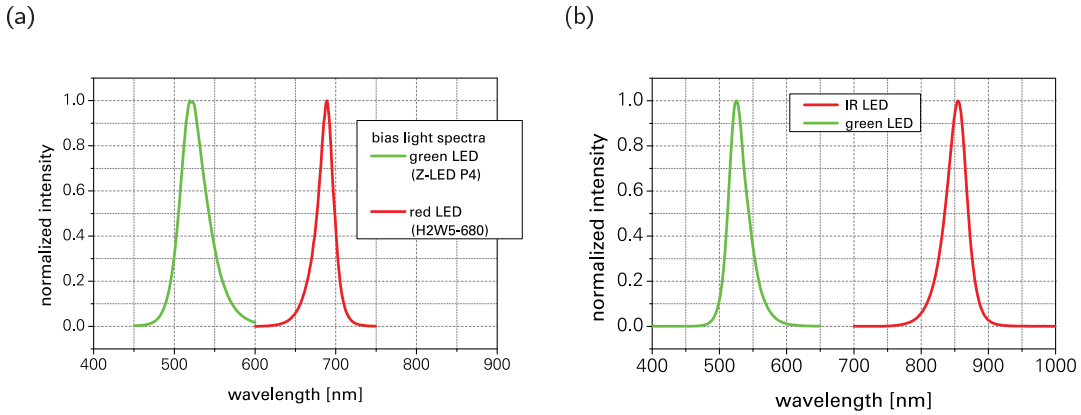

Fig. S15: *Spectra of the bias light sources for SR measurement at (a) TUD and (b) ISE.*

provided by LEDs. For the presented measurements red (H2W5-680, Roithner Lasertechnik, Vienna, Austria) and green (Z-LED P4, Seoul Semiconductors, Korea) LEDs with nominal emission peaks at 680nm (22nm FWHM) and 525nm (45nm FWHM), respectively, were used. The measured spectra are shown in Fig. S15. The intensity of the bias light was 8.9mW/cm^2 and 6.3 for the green and the red LED, respectively. The electrical bias over the tandem cell was provided by the lock-in-amplifier. The test cell was measured using an aperture with a size of 2.89mm^2.

The differential spectral response measurements at TUe were done in a home-built set-up. The modulated monochromatic (Oriel Cornerstone 130 1/8 m, Newport) probe light (Halotone halogen lamp, Philips) was mechanically chopped at a frequency of 165Hz with an optical chopper (SR 540, Stanford Research). The bias illumination was provided by a 532nm (B&W, Tek Inc., 30mW) and 780nm (B&W, Tek Inc., 21mW) solid state laser. The sample was illuminated through an aperture of 2mm^2 which is smaller than the device area to avoid errors. The measurements were performed with a lock-in-amplifier (SR 830, Stanford Research) over a load of 50Ω. All data was recorded by a Labview program on a computer. The electrical bias over the tandem cell was provided by the lock-in-amplifier.

For the differential spectral response measurement at Fraunhofer ISE CalLab PV Cells, Freiburg, a grating double monochromator with an Xenon arc lamp was used. The quasimonochromatic light was chopped by a mechanical chopper with a frequency of 173Hz and had a spectral bandwidth below 10nm. Its intensity was recorded by a silicon or a germanium monitor solar cell, depending on the wavelength range. The modulated signals of test and monitor cells were converted by home-built current-voltage-amplifiers with measurement resistors adaptable to the signal intensity. The voltage biasing of the test cell was provided by the current-voltage-amplifier as well. The simultaneous recording of test and monitor cell signal was done with two signal recovery lock-in amplifiers and the results were used for the correction of fluctuations of the Xe arc lamp. For bias light illumination several LED and halogen light sources with appropriate absorption and interference filters were used. The calibration of the system was done with unfiltered WPVS reference cells, primary calibrated by Physikalisch Technische Bundesanstalt (PTB) Braunschweig. The spot size of the monochromatic light is smaller than the test- and reference solar cell. The cell is aspirated to a temperature controlled measurement chuck and kept at 25°C during the measurement.

The *JV*-measurements at TUD are carried out using a class A sun simulator (16S-150 V.3 by Solar Light and Co., USA) in combination with neutral density filters for different orders of magnitude of intensity . The light is coupled into a glass fiber (Spectral Products, Putnam, USA) and the current of the test device is measured with a Keithley 2400 Source Measurement Unit (Keithley Instruments Inc., USA). The intensity at the test cell position is monitored by a Hamamatsu S1337-33BQ Si-photodiode (Hamamatsu Photonics K.K., Japan) being calibrated with an aperture mask with an area of 2.966mm^2 at the Fraunhofer ISE CalLab, Germany. The wavelength range of the spectral response of the used Si-diode is suitable for both subcells. The illumination spectrum

at the output of the fiber is controlled with a CAS140T spectrometer (Instrument Systems, Munich, Germany). The test cell is measured without aperture and the device area is assumed to be the overlap of ITO, organic layers and metal contact. The measurement setup as well as the data recording is controlled by a custom-made LabView program. For the determination of the spectrometric characterization, an extended setup with a bifurcated glass fiber (Loptek GmbH & Co. KG, Germany) is used to couple a white LED (LUXEON K2 LXK2-PWC4-0220, Philips Lumiled, San Jose, USA) as second light source into the second port of the glass fiber. Additionally, a long pass filter ($T = 0.5$ at 600nm) was applied to the first port of the glass fiber to reduce the spectral overlap of both light sources. The spectra of the sun simulator with and without applied long pass filter, of the LED serving as second light source as well as the resulting illumination spectra used for spectrometric characterization are shown in Fig. S16.

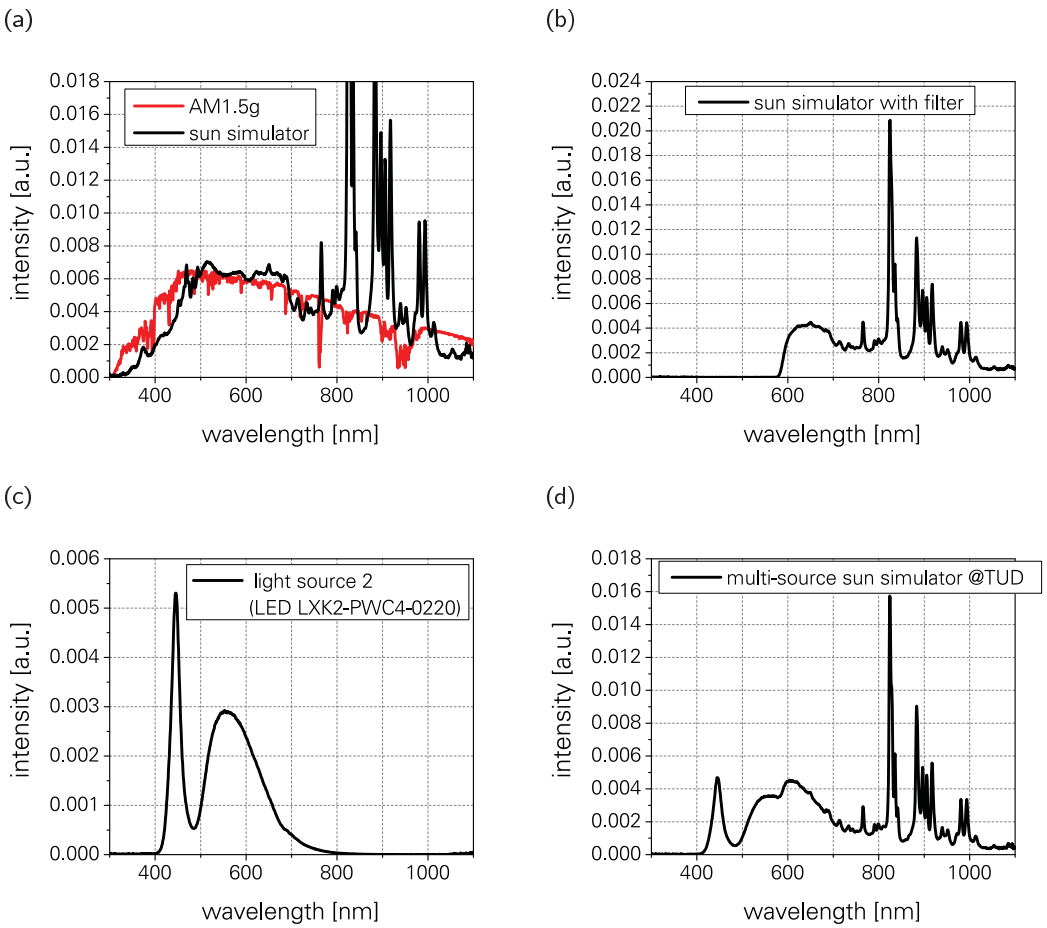

Fig. S16: *Spectra of the light sources used for JV-measurements at TUD: (a) sun simulator used as single-source sun simulator together with the AM1.5g reference spectrum for comparison[79], (b) sun simulator with applied long pass filter ($T = 0.5$ at 600 nm) as used as first light source of a multi-source sun simulator, (c) white LED (Philips LUXEON K2 LXK2-PWC4-0220) used as second light source for realizing a multi-source sun simulator and (d) the resulting spectrum of the multi-source sun simulator for the metric point (1,1).*

For the measurement of the current-voltage characteristics at ISE a homebuilt multi-source solar simulator is used. This has a Xenon arc lamp and two differently filtered halogen lamp fields that can be adjusted in intensity separately. Their spectra for the metric point (1,1) are shown

DOI: 10.1038/NPHOTON.2015.124

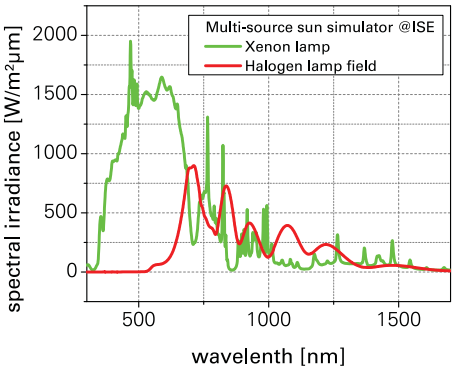

Fig. 17: *Spectra of the light sources of the multi-source sun simulator used for the spectral metric determination at ISE.*

in Fig. 17. The spectra and homogeneities of the different sources are measured within certain time intervals at several points of the whole intensity range of each source. With the determined spectral response data the intensities for all light sources are calculated and set according to a primary calibrated reference solar cell (PTB). For organic tandem cells only the Xe lamp and one of the halogen lamp fields are used. The variable load for the *JV*-characteristics is a Kepco bipolar power supply. The voltage and the current of the solar cell are recorded by multimeters and adaptable shunt resistors. The solar cell under test is aspirated to a temperature controlled measurement chuck and kept at 25°C. The measurement was performed without aperture.

Calculations of optical interference effects are carried out using a simulation program based on the transfer matrix formalism. The details of the simulation procedure are described in reference[113]. The optical constants of the organic materials and the blend layers are extracted from reflection and transmission measurements on films of the accordant materials and blends with different known layer thicknesses.

7 Bibliography

References

[1] J. You, L. Dou, K. Yoshimura, T. Kato, K. Ohya, T. Moriarty, K. Emery, C.-C. Chen, J. Gao, G. Li, Y. Yang, *A polymer tandem solar cell with 10.6% power conversion efficiency*, Nat. Commun. 4 p. 1446, 2013, doi: 10.1038/ncomms2411

[2] M. A. Green, K. Emery, Y. Hishikawa, W. Warta, E. D. Dunlop, *Solar cell efficiency tables (version 44)*, Prog. Photovolt: Res. Appl. 22 (7) p. 701, 2014, doi: 10.1002/pip.2525

[3] *ASTM E2236-10, Standard Test Methods for Measurement of Electrical Performance and Spectral Response of Nonconcentrator Multijunction Photovoltaic Cells and Modules*, ASTM International, West Conshohocken, PA, 2010, doi: 10.1520/E2236-10

[4] M. Riede, C. Uhrich, J. Widmer, R. Timmreck, D. Wynands, G. Schwartz, W.-M. Gnehr, D. Hildebrandt, A. Weiss, J. Hwang, S. Sundarraj, P. Erk, M. Pfeiffer, K. Leo, *Efficient organic tandem solar cells based on small molecules*, Adv. Funct. Mater. 21 (16) p. 3019, 2011, doi: 10.1002/adfm.201002760

[5] L. Dou, J. You, J. Yang, C.-C. Chen, Y. He, S. Murase, T. Moriarty, K. Emery, G. Li, Y. Yang, *Tandem polymer solar cells featuring a spectrally matched low-bandgap polymer*, Nat. Photonics 6 (3) p. 180, 2012, doi: 10.1038/NPHOTON.2011.356

[6] S. Albrecht, B. Grootoonk, S. Neubert, S. Roland, J. Wordenweber, M. Meier, R. Schlatmann, A. Gordijn, D. Neher, *Efficient hybrid inorganic/organic tandem solar cells with tailored recombination contacts*, Sol. Energy Mater. Sol. Cells 127 p. 157, 2014, doi: 10.1016/j.solmat.2014.04.020

[7] M. J. Speirs, B. G. H. M. Groeneveld, L. Protesescu, C. Piliego, M. V. Kovalenko, M. A. Loi, *Hybrid inorganic-organic tandem solar cells for broad absorption of the solar spectrum*, Phys. Chem. Chem. Phys. 16 (17) p. 7672, 2014, doi: 10.1039/c4cp00846d

[8] J.-H. Kim, S. A. Shin, J. B. Park, C. E. Song, W. S. Shin, H. Yang, Y. Li, D.-H. Hwang, *Fluorinated benzoselenadiazole-based low-band-gap polymers for high efficiency inverted single and tandem organic photovoltaic cells*, Macromolecules 47 (5) p. 1613, 2014, doi: 10.1021/ma4026493

[9] J.-H. Kim, C. E. Song, B. Kim, I.-N. Kang, W. S. Shin, D.-H. Hwang, *Thieno[3,2-b]thiophene-substituted benzo[1,2-b:4,5-b ']dithiophene as a promising building block for low bandgap semiconducting polymers for high-performance single and tandem organic photovoltaic cells*, Chem. Mater. 26 (2) p. 1234, 2014, doi: 10.1021/cm4035903

[10] E. Y. Kim, S. Yu, J. H. Moon, S. M. Yoo, C. Kim, H. K. Kim, W. I. Lee, *Formation of double-layered TiO_2 structures with selectively-positioned molecular dyes for efficient flexible dye-sensitized solar cells*, Electrochim. Acta 111 p. 261, 2013, doi: 10.1016/j.electacta.2013.08.081

[11] Y. Liu, C.-C. Chen, Z. Hong, J. Gao, Y. M. Yang, H. Zhou, L. Dou, G. Li, Y. Yang, *Solution-processed small-molecule solar cells: breaking the 10% power conversion efficiency*, Sci. Rep. 3 p. 3356, 2013, doi: 10.1038/srep03356

[12] M. Reinhard, P. Sonntag, R. Eckstein, L. Buerkert, A. Bauer, B. Dimmler, U. Lemmer, A. Colsmann, *Monolithic hybrid tandem solar cells comprising copper indium gallium diselenide and organic subcells*, Appl. Phys. Lett. 103 (14) p. 143904, 2013, doi: 10.1063/1.4824017

[13] K. Li, Z. Li, K. Feng, X. Xu, L. Wang, Q. Peng, *Development of large band-gap conjugated copolymers for efficient regular single and tandem organic solar cells*, J. Am. Chem. Soc. 135 (36) p. 13549, 2013, doi: 10.1021/ja406220a

[14] T. Kim, Y.-S. Kim, J. Y. Choi, J. H. Jeon, W. W. Park, S. W. Moon, S.-M. Kim, S. Han, B. Kim, D.-K. Lee, H. Kim, J. Y. Kim, M. J. Ko, K. Kim, *Reversed organic-inorganic hybrid tandem solar cells for improved interfacial series resistances and balanced photocurrents*, Synth. Met. 175 p. 103, 2013, doi: 10.1016/j.synthmet.2013.05.002

[15] N. Ishiyama, M. Kubo, T. Kaji, M. Hiramoto, *Tandem organic solar cells formed in co-deposited films by doping*, Org. Electron. 14 (7) p. 1793, 2013, doi: 10.1016/j.orgel.2013.04.003

[16] S. Pattnaik, T. Xiao, R. Shinar, J. Shinar, V. L. Dalal, *Novel hybrid amorphous/organic tandem junction solar cell*, IEEE J. Photovolt. 3 (1) p. 295, 2013, doi: 10.1109/JPHOTOV.2012.2212700

[17] Z. Tang, Z. George, Z. Ma, J. Bergqvist, K. Tvingstedt, K. Vandewal, E. Wang, L. M. Andersson, M. R. Andersson, F. Zhang, O. Inganäs, *Semi-transparent tandem organic solar cells with 90% internal quantum efficiency*, Adv. Energy Mater. 2 (12) p. 1467, 2012, doi: 10.1002/aenm.201200204

[18] J. H. Seo, D.-H. Kim, S.-H. Kwon, M. Song, M.-S. Choi, S. Y. Ryu, H. W. Lee, Y. C. Park, J.-D. Kwon, K.-S. Nam, Y. Jeong, J.-W. Kang, C. S. Kim, *High efficiency inorganic/organic hybrid tandem solar cells*, Adv. Mater. 24 (33) p. 4523, 2012, doi: 10.1002/adma.201201419

[19] J. Yang, W. Chen, B. Yu, H. Wang, D. Yan, *Organic tandem solar cell using active interconnecting layer*, Org. Electron. 13 (6) p. 1018, 2012, doi: 10.1016/j.orgel.2012.02.015

DOI: 10.1038/NPHOTON.2015.124

[20] W. Chen, X. Qiao, J. Yang, B. Yu, D. Yan, *Efficient broad-spectrum parallel tandem organic solar cells based on the highly crystalline chloroaluminum phthalocyanine films as the planar layer*, Appl. Phys. Lett. 100 (13) p. 133302, 2012, doi: 10.1063/1.3697397

[21] J. Meiss, T. Menke, K. Leo, C. Uhrich, W.-M. Gnehr, S. Sonntag, M. Pfeiffer, M. Riede, *Highly efficient semitransparent tandem organic solar cells with complementary absorber materials*, Appl. Phys. Lett. 99 (4) p. 043301, 2011, doi: 10.1063/1.3610551

[22] L. Li, Y. Hao, X. Yang, J. Zhao, H. Tian, C. Teng, A. Hagfeldt, L. Sun, *A double-band tandem organic dye-sensitized solar cell with an efficiency of 11.5%*, Chemsuschem 4 (5) p. 609, 2011, doi: 10.1002/cssc.201100002

[23] A. P. Yuen, A.-M. Hor, J. S. Preston, R. Klenkler, N. M. Bamsey, R. O. Loutfy, *A simple parallel tandem organic solar cell based on metallophthalocyanines*, Appl. Phys. Lett. 98 (17) p. 173301, 2011, doi: 10.1063/1.3579250

[24] D. W. Zhao, L. Ke, Y. Li, S. T. Tan, A. K. K. Kyaw, H. V. Demir, X. W. Sun, D. L. Carroll, G. Q. Lo, D. L. Kwong, *Optimization of inverted tandem organic solar cells*, Sol. Energy Mater. Sol. Cells 95 (3) p. 921, 2011, doi: 10.1016/j.solmat.2010.11.023

[25] D. Cheyns, B. P. Rand, P. Heremans, *Organic tandem solar cells with complementary absorbing layers and a high open-circuit voltage*, Appl. Phys. Lett. 97 (3) p. 033301, 2010, doi: 10.1063/1.3464169

[26] T. Taima, T. Yamanari, J. Sakai, Y. Yoshida, *Tandem organic photovoltaic cells based on low-molecular-weight semiconductors*, Jpn. J. Appl. Phys. 49 (1) p. 01AC04, 2010, doi: 10.1143/JJAP.49.01AC04

[27] I. Bruder, M. Karlsson, F. Eickemeyer, J. Hwang, P. Erk, A. Hagfeldt, J. Weis, N. Pschirer, *Efficient organic tandem cell combining a solid state dye-sensitized and a vacuum deposited bulk heterojunction solar cell*, Sol. Energy Mater. Sol. Cells 93 (10) p. 1896, 2009, doi: 10.1016/j.solmat.2009.05.020

[28] S. Tanaka, K. Mielczarek, R. Ovalle-Robles, B. Wang, D. Hsu, A. A. Zakhidov, *Monolithic parallel tandem organic photovoltaic cell with transparent carbon nanotube interlayer*, Appl. Phys. Lett. 94 (11) p. 113506, 2009, doi: 10.1063/1.3095594

[29] J. Liu, S. Shao, G. Fang, J. Wang, B. Meng, Z. Xie, L. Wang, *High-efficiency inverted tandem polymer solar cells with step-Al-doped MoO_3 interconnection layer*, Sol. Energy Mater. Sol. Cells 120 p. 744, 2014, doi: 10.1016/j.solmat.2013.06.034

[30] X. Fan, S. Guo, G. Fang, C. Zhan, H. Wang, Z. Zhang, Y. Li, *An efficient PDPPTPT:PC_{61}BM-based tandem polymer solar cells with a Ca/Ag/MoO_3 intermediate layer*, Sol. Energy Mater. Sol. Cells 113 p. 135, 2013, doi: 10.1016/j.solmat.2013.02.008

[31] W. Li, A. Furlan, K. H. Hendriks, M. M. Wienk, R. A. J. Janssen, *Efficient tandem and triple-junction polymer solar cells*, J. Am. Chem. Soc. 135 (15) p. 5529, 2013, doi: 10.1021/ja401434x

[32] S. Kouijzer, S. Esiner, C. H. Frijters, M. Turbiez, M. M. Wienk, R. A. J. Janssen, *Efficient inverted tandem polymer solar cells with a solution-processed recombination layer*, Adv. Energy Mater. 2 (8) p. 945, 2012, doi: 10.1002/aenm.201100773

[33] V. S. Gevaerts, A. Furlan, M. M. Wienk, M. Turbiez, R. A. J. Janssen, *Solution processed polymer tandem solar cell using efficient small and wide bandgap polymer:fullerene blends*, Adv. Mater. 24 (16) p. 2130, 2012, doi: 10.1002/adma.201104939

[34] J. Yang, J. You, C.-C. Chen, W.-C. Hsu, H.-R. Tan, X. W. Zhang, Z. Hong, Y. Yang, *Plasmonic polymer tandem solar cell*, ACS Nano 5 (8) p. 6210, 2011, doi: 10.1021/nn202144b

[35] J. Yang, R. Zhu, Z. Hong, Y. He, A. Kumar, Y. Li, Y. Yang, *A robust inter-connecting layer for achieving high performance tandem polymer solar cells*, Adv. Mater. 23 (30) p. 3465, 2011, doi: 10.1002/adma.201100221

[36] C.-H. Chou, W. L. Kwan, Z. Hong, L.-M. Chen, Y. Yang, *A metal-oxide interconnection layer for polymer tandem solar cells with an inverted architecture*, Adv. Mater. 23 (10) p. 1282, 2011, doi: 10.1002/adma.201001033

[37] J. Gilot, M. M. Wienk, R. A. J. Janssen, *Optimizing polymer tandem solar cells*, Adv. Mater. 22 (8) p. E67, 2010, doi: 10.1002/adma.200902398

[38] S. Sista, M.-H. Park, Z. Hong, Y. Wu, J. Hou, W. L. Kwan, G. Li, Y. Yang, *Highly efficient tandem polymer photovoltaic cells*, Adv. Mater. 22 (3) p. 380, 2010, doi: 10.1002/adma.200901624

[39] A. R. b. M. Yusoff, D. Kim, H. P. Kim, F. K. Shneider, W. J. da Silva, J. Jang, *High efficiency solution processed polymer inverted triple-junction solar cell exhibiting conversion efficiency of 11.83%*, Energy Environ. Sci. accepted, 2014, doi: 10.1039/C4EE03048F

[40] H.-S. Shim, J.-H. Chang, C.-I. Wub, J.-J. Kim, *Effect of different p-dopants in an interconnection unit on the performance of tandem organic solar cells*, Org. Electron. 15 (8) p. 1805, 2014, doi: 10.1016/j.orgel.2014.04.033

[41] Z. Ke-Ning, Y. Li-Ying, C. Huan-Qi, Q. Wen-Jing, Y. Shou-Gen, *A simple interconnection layer for tandem organic solar cells with improved efficiency and fill factor*, Chin. Phys. Lett. 31 (6) p. 068801, 2014, doi: 10.1088/0256-307X/31/6/068801

[42] H.-S. Shim, J.-H. Chang, S.-J. Yoo, C.-I. Wu, J.-J. Kim, *Correlation of the electronic structure of an interconnection unit with the device performance of tandem organic solar cells*, J. Mater. Chem. 2 (15) p. 5450, 2014, doi: 10.1039/c3ta14628f

[43] D. Y. Luo, L. M. Yu, J. X. Man, Z. Liu, Z. H. Lu, *A nanocomposite interconnecting layer for tandem small molecular organic photovoltaic cells*, Appl. Phys. Lett. 104 (12) p. 123301, 2014, doi: 10.1063/1.4869354

[44] B. Lechene, G. Perrier, K. Emmanouil, S. Kennou, B. Bouthinon, R. de Bettignies, *Design of intermediate layers for solution-processed tandem organic solar cells: Guidelines from a case study on TiO_x and ZnO*, Sol. Energy Mater. Sol. Cells 120 p. 709, 2014, doi: 10.1016/j.solmat.2013.08.032

[45] N. Li, D. Baran, K. Forberich, F. Machui, T. Ameri, M. Turbiez, M. Carrasco-Orozco, M. Drees, A. Facchetti, F. C. Krebs, C. J. Brabec, *Towards 15% energy conversion efficiency: a systematic study of the solution-processed organic tandem solar cells based on commercially available materials*, Energy Environ. Sci. 6 (12) p. 3407, 2013, doi: 10.1039/c3ee42307g

[46] A. R. b. M. Yusoff, W. J. da Silva, H. P. Kim, J. Jang, *Extremely stable all solution processed organic tandem solar cells with TiO_2/GO recombination layer under continuous light illumination*, Nanoscale 5 (22) p. 11051, 2013, doi: 10.1039/c3nr03068g

[47] E. New, T. Howells, P. Sullivan, T. S. Jones, *Small molecule tandem organic photovoltaic cells incorporating an α-NPD optical spacer layer*, Org. Electron. 14 (9) p. 2353, 2013, doi: 10.1016/j.orgel.2013.05.037

[48] J.-H. Kim, C. E. Song, H. U. Kim, A. C. Grimsdale, S.-J. Moon, W. S. Shin, S. K. Choi, D.-H. Hwang, *High open circuit voltage solution-processed tandem organic photovoltaic cells employing a bottom cell using a new medium band gap semiconducting polymer*, Chem. Mater. 25 (13) p. 2722, 2013, doi: 10.1021/cm401527b

[49] W. Nie, R. C. Coffin, D. L. Carroll, *Silver nanoparticle-doped titanium oxide thin films for intermediate layers in organic tandem solar cell*, Int. J. Photoenergy 829463, 2013, doi: 10.1155/2013/829463

DOI: 10.1038/NPHOTON.2015.124

[50] Y. Zhou, C. Fuentes-Hernandez, J. W. Shim, T. M. Khan, B. Kippelen, *High performance polymeric charge recombination layer for organic tandem solar cells*, Energy Environ. Sci. 5 (12) p. 9827, 2012, doi: 10.1039/c2ee23294d

[51] A. Puetz, F. Steiner, J. Mescher, M. Reinhard, N. Christ, D. Kutsarov, H. Kalt, U. Lemmer, A. Colsmann, *Solution processable, precursor based zinc oxide buffer layers for 4.5% efficient organic tandem solar cells*, Org. Electron. 13 (11) p. 2696, 2012, doi: 10.1016/j.orgel.2012.07.043

[52] J. Li, Q.-Y. Bao, H.-X. Wei, Z.-Q. Xu, J.-P. Yang, Y.-Q. Li, S.-T. Lee, J.-X. Tang, *Role of transition metal oxides in the charge recombination layer used in tandem organic photovoltaic cells*, J. Mater. Chem. 22 (13) p. 6285, 2012, doi: 10.1039/c2jm30272a

[53] S. W. Tong, Y. Wang, Y. Zheng, M.-F. Ng, K. P. Loh, *Graphene intermediate layer in tandem organic photovoltaic cells*, Adv. Funct. Mater. 21 (23) p. 4430, 2011, doi: 10.1002/adfm.201101376

[54] D. Lee, W. K. Bae, I. Park, D. Y. Yoon, S. Lee, C. Lee, *Transparent electrode with ZnO nanoparticles in tandem organic solar cells*, Sol. Energy Mater. Sol. Cells 95 (1) p. 365, 2011, doi: 10.1016/j.solmat.2010.04.020

[55] J. Y. Kim, S. Noh, D. Lee, C. Lee, *Organic tandem solar cell using a semi-transparent top electrode for both-side light absorption*, J. Korean Phys. Soc. 57 (6) p. 1852, 2010, doi: 10.3938/jkps.57.1852

[56] X. W. Sun, D. W. Zhao, L. Ke, A. K. K. Kyaw, G. Q. Lo, D. L. Kwong, *Inverted tandem organic solar cells with a MoO3/Ag/Al/Ca intermediate layer*, Appl. Phys. Lett. 97 (5) p. 053303, 2010, doi: 10.1063/1.3469928

[57] R. Timmreck, S. Olthof, K. Leo, M. Riede, *Highly doped layers as efficient electron-hole recombination contacts for tandem organic solar cells*, J. Appl. Phys. 108 (3) p. 033108, 2010, doi: 10.1063/1.3467786

[58] D. J. D. Moet, P. de Bruyn, P. W. M. Blom, *High work function transparent middle electrode for organic tandem solar cells*, Appl. Phys. Lett. 96 (15) p. 153504, 2010, doi: 10.1063/1.3387863

[59] B. J. Lee, H. J. Kim, W.-I. Jeong, J.-J. Kim, *A transparent conducting oxide as an efficient middle electrode for flexible organic tandem solar cells*, Sol. Energy Mater. Sol. Cells 94 (3) p. 542, 2010, doi: 10.1016/j.solmat.2009.11.021

[60] J. Sakai, K. Kawano, T. Yamanari, T. Taima, Y. Yoshida, A. Fujii, M. Ozaki, *Efficient organic photovoltaic tandem cells with novel transparent conductive oxide interlayer and poly-(3-hexylthiophene): Fullerene active layers*, Sol. Energy Mater. Sol. Cells 94 (2) p. 376, 2010, doi: 10.1016/j.solmat.2009.08.008

[61] S. J. Kim, W. J. Kim, A. N. Cartwright, P. N. Prasad, *Self-passivating hybrid (organic/inorganic) tandem solar cell*, Sol. Energy Mater. Sol. Cells 93 (5) p. 657, 2009, doi: 10.1016/j.solmat.2008.12.011

[62] D. Gupta, M. M. Wienk, R. A. J. Janssen, *Indium tin oxide-free tandem polymer solar cells on opaque substrates with top illumination*, ACS Appl. Mater. Interfaces 6 (16) p. 13937, 2014, doi: 10.1021/am503262e

[63] A. R. b. M. Yusoff, S. J. Lee, J. Kim, F. K. Shneider, W. J. da Silva, J. Jang, *High-performance inverted tandem polymer solar cells utilizing thieno[3,4-c]pyrrole-4,6-dione copolymer*, ACS Appl. Mater. Interfaces 6 (15) p. 13079, 2014, doi: 10.1021/am5029318

[64] A. R. b. M. Yusoff, S. J. Lee, H. P. Kim, F. K. Shneider, W. J. da Silva, J. Jang, *8.91% power conversion efficiency for polymer tandem solar cells*, Adv. Funct. Mater. 24 (15) p. 2240, 2014, doi: 10.1002/adfm.201303471

[65] P.-N. Yeh, T.-H. Jen, Y.-S. Cheng, S.-A. Chen, *Large active area inverted tandem polymer solar cell with high performance via insertion of subnano-scale silver layer*, Sol. Energy Mater. Sol. Cells 120 p. 728, 2014, doi: 10.1016/j.solmat.2013.07.007

[66] J. Jo, J.-R. Pouliot, D. Wynands, S. D. Collins, J. Y. Kim, T. L. Nguyen, H. Y. Woo, Y. Sun, M. Leclerc, A. J. Heeger, *Enhanced efficiency of single and tandem organic solar cells incorporating a diketopyrrolopyrrole-based low-bandgap polymer by utilizing combined ZnO/polyelectrolyte electron-transport layers*, Adv. Mater. 25 (34) p. 4783, 2013, doi: 10.1002/adma.201301288

[67] C.-C. Chen, L. Dou, J. Gao, W.-H. Chang, G. Li, Y. Yang, *High-performance semitransparent polymer solar cells possessing tandem structures*, Energy Environ. Sci. 6 (9) p. 2714, 2013, doi: 10.1039/c3ee40860d

[68] Y.-L. Chen, W.-S. Kao, C.-E. Tsai, Y.-Y. Lai, Y.-J. Cheng, C.-S. Hsu, *A new ladder-type benzodi(cyclopentadithiophene)-based donor-acceptor polymer and a modified hole-collecting PEDOT:PSS layer to achieve tandem solar cells with an open-circuit voltage of 1.62 V*, Chem. Commun. 49 (70) p. 7702, 2013, doi: 10.1039/c3cc43756f

[69] J. You, C.-C. Chen, Z. Hong, K. Yoshimura, K. Ohya, R. Xu, S. Ye, J. Gao, G. Li, Y. Yang, *10.2% power conversion efficiency polymer tandem solar cells consisting of two identical sub-cells*, Adv. Mater. 25 (29) p. 3973, 2013, doi: 10.1002/adma.201300964

[70] E. Lee, J. Kim, C. Kim, *Polymer tandem photovoltaic cells with molecularly intimate interfaces achieved by a thin-film transfer technique*, Sol. Energy Mater. Sol. Cells 105 p. 1, 2012, doi: 10.1016/j.solmat.2012.05.025

[71] R. Schueppel, R. Timmreck, N. Allinger, T. Mueller, M. Furno, C. Uhrich, K. Leo, M. Riede, *Controlled current matching in small molecule organic tandem solar cells using doped spacer layers*, J. Appl. Phys. 107 (4) p. 044503, 2010, doi: 10.1063/1.3277051

[72] S. K. Hau, H.-L. Yip, K.-S. Chen, J. Zou, A. K.-Y. Jen, *Solution processed inverted tandem polymer solar cells with self-assembled monolayer modified interfacial layers*, Appl. Phys. Lett. 97 (25) p. 253307, 2010, doi: 10.1063/1.3530431

[73] X. Guo, F. Liu, B. Meng, Z. Xie, L. Wang, *Efficient tandem polymer photovoltaic cells using inorganic metal oxides as a transparent middle connection unit*, Org. Electron. 11 (7) p. 1230, 2010, doi: 10.1016/j.orgel.2010.05.004

[74] F.-C. Chen, C.-H. Lin, *Construction and characteristics of tandem organic solar cells featuring small molecule-based films on polymer-based subcells*, J. Phys. D: Appl. Phys. 43 (2) p. 025104, 2010, doi: 10.1088/0022-3727/43/2/025104

[75] B. E. Lassiter, J. D. Zimmerman, S. R. Forrest, *Tandem organic photovoltaics incorporating two solution-processed small molecule donor layers*, Appl. Phys. Lett. 103 (12) p. 123305, 2013, doi: 10.1063/1.4821112

[76] *IEC 60904-3, Photovoltaic devices - Part 3: Measurement principles for terrestrial photovoltaic (PV) solar devices with reference spectral irradiance data*, International Standard, International Electrotechnical Comission, Geneva, Switzerland, 2008

[77] *ISO 15387, Space systems - Space solar cells - Requirements, measurements and calibration procedures*, International Standard, International Organization for Standardization, Geneva, Switzerland, 2005

[78] *IEC 62670-1, Photovoltaic concentrators (CPV) - Part 1: Performance testing Standard conditions*, International Standard, International Electrotechnical Comission, Geneva, Switzerland, 2013

DOI: 10.1038/NPHOTON.2015.124

[79] *ASTM G173-03 (2012), Standard Tables for Reference Solar Spectral Irradiances: Direct Normal and Hemispherical on 37° Tilted Surface*, ASTM International, West Conshohocken, PA, 2012, doi: 10.1520/G0173-03R12

[80] *IEC 60904-7, Photovoltaic devices - Part 7: Computation of the spectral mismatch correction for measurements of photovoltaic devices*, International Standard, International Electrotechnical Comission, Geneva, Switzerland, 2008

[81] *ASTM E973-10, Standard Test Method for Determination of the Spectral Mismatch Parameter Between a Photovoltaic Device and a Photovoltaic Reference Cell*, ASTM International, West Conshohocken, PA, 2010, doi: 10.1520/E0973-10

[82] C. H. Seaman, *Calibration of solar-cells by the reference cell method - the spectral mismatch problem*, Sol. Energy 29 (4) p. 291, 1982, doi: 10.1016/0038-092X(82)90244-4

[83] *IEC 60904-9, Photovoltaic devices - Part 9: Solar simulator performance requirements*, International Standard, International Electrotechnical Comission, Geneva, Switzerland, 2007

[84] *ASTM E927-10, Solar Simulation for Photovoltaic Testing*, ASTM International, West Conshohocken, PA, 2010, doi: 10.1520/E0927-10

[85] *IEC 60904-1, Photovoltaic devices - Part 1: Measurement of photovoltaic current-voltage characteristics*, International Standard, International Electrotechnical Comission, Geneva, Switzerland, 2006

[86] *ASTM E948-15, Standard Test Method for Electrical Performance of Photovoltaic Cells Using Reference Cells Under Simulated Sunlight*, ASTM International, West Conshohocken, PA, 2015, doi: 10.1520/E0948-15

[87] M. Meusel, R. Adelhelm, F. Dimroth, A. W. Bett, W. Warta, *Spectral mismatch correction and spectrometric characterization of monolithic III-V multi-junction solar cells*, Prog. Photovolt: Res. Appl. 10 (4) p. 243, 2002, doi: 10.1002/pip.407

[88] J. Gilot, M. M. Wienk, R. A. J. Janssen, *Measuring the external quantum efficiency of two-terminal polymer tandem solar cells*, Adv. Funct. Mater. 20 (22) p. 3904, 2010, doi: 10.1002/adfm.201001167

[89] R. Timmreck, K. Leo, M. Riede, *Characterization of tandem organic solar cells comprising subcells of identical absorber material*, Prog. Photovolt: Res. Appl. accepted, 2014, doi: 10.1002/pip.2541

[90] J. Gilot, M. M. Wienk, R. A. J. Janssen, *Measuring the current density - voltage characteristics of individual subcells in two-terminal polymer tandem solar cells*, Org. Electron. 12 (4) p. 660, 2011, doi: 10.1016/j.orgel.2011.01.014

[91] J. Metzdorf, *Calibration of solar-cells. 1: the differential spectral responsivity method*, Appl. Opt. 26 (9) p. 1701, 1987, doi: 10.1364/AO.26.001701

[92] J. Metzdorf, W. Moller, T. Wittchen, D. Hunerhoff, *Principle and application of differential spectroradiometry*, Metrologia 28 (3) p. 247, 1991, doi: 10.1088/0026-1394/28/3/028

[93] D. J. Wehenkel, K. H. Hendriks, M. M. Wienk, R. A. J. Janssen, *The effect of bias light on the spectral responsivity of organic solar cells*, Org. Electron. 13 (12) p. 3284, 2012, doi: 10.1016/j.orgel.2012.09.040

[94] T. Mueller, R. Gresser, K. Leo, M. Riede, *Organic solar cells based on a novel infrared absorbing aza-bodipy dye*, Sol. Energy Mater. Sol. Cells 99 p. 176, 2012, doi: 10.1016/j.solmat.2011.11.006

[95] D. Wynands, M. Levichkova, M. Riede, M. Pfeiffer, P. Baeuerle, R. Rentenberger, P. Denner, K. Leo, *Correlation between morphology and performance of low bandgap oligothiophene:C_{60} mixed heterojunctions in organic solar cells*, J. Appl. Phys. 107 (1) p. 014517, 2010, doi: 10.1063/1.3271407

[96] M. Meusel, C. Baur, G. Letay, A. W. Bett, W. Warta, E. Fernandez, *Spectral response measurements of monolithic GaInP/Ga(In)As/Ge triple-junction solar cells: Measurement artifacts and their explanation*, Prog. Photovolt: Res. Appl. 11 (8) p. 499, 2003, doi: 10.1002/pip.514

[97] V. Shrotriya, G. Li, Y. Yao, T. Moriarty, K. Emery, Y. Yang, *Accurate measurement and characterization of organic solar cells*, Adv. Funct. Mater. 16 (15) p. 2016, 2006, doi: 10.1002/adfm.200600489

[98] S. Ito, M. K. Nazeeruddin, P. Liska, P. Comte, R. Charvet, P. Pechy, M. Jirousek, A. Kay, S. M. Zakeeruddin, M. Gratzel, *Photovoltaic characterization of dye-sensitized solar cells: Effect of device masking on conversion efficiency*, Prog. Photovoltics 14 (7) p. 589, 2006, doi: 10.1002/pip.683

[99] A. Cravino, P. Schilinsky, C. J. Brabec, *Characterization of organic solar cells: the importance of device layout*, Adv. Funct. Mater. 17 (18) p. 3906, 2007, doi: 10.1002/adfm.200700295

[100] S. A. Gevorgyan, J. E. Carle, R. Sondergaard, T. T. Larsen-Olsen, M. Jorgensen, F. C. Krebs, *Accurate characterization of OPVs: Device masking and different solar simulators*, Sol. Energy Mater. Sol. Cells 110 p. 24, 2013, doi: 10.1016/j.solmat.2012.11.020

[101] E. Zimmermann, P. Ehrenreich, T. Pfadler, J. A. Dorman, J. Weickert, L. Schmidt-Mende, *Erroneous efficiency reports harm organic solar cell research*, Nat. Photonics 8 p. 669, 2014, doi: 10.1038/nphoton.2014.210

[102] D. J. Wehenkel, L. J. A. Koster, M. M. Wienk, R. A. J. Janssen, *Influence of injected charge carriers on photocurrents in polymer solar cells*, Phys. Rev. B 85 (12) p. 125203, 2012, doi: 10.1103/PhysRevB.85.125203

[103] J. Meiss, M. K. Riede, K. Leo, *Optimizing the morphology of metal multilayer films for indium tin oxide (ITO)-free inverted organic solar cells*, J. Appl. Phys. 105 (6) p. 063108, 2009, doi: 10.1063/1.3100039

[104] J. Meiss, K. Leo, M. K. Riede, C. Uhrich, W.-M. Gnehr, S. Sonntag, M. Pfeiffer, *Efficient semitransparent small-molecule organic solar cells*, Appl. Phys. Lett. 95 (21) p. 213306, 2009, doi: 10.1063/1.3268784

[105] K.-S. Lee, I. Kim, C. B. Yeon, J. W. Lim, S. J. Yun, G. E. Jabbour, *Thin metal electrodes for semitransparent organic photovoltaics*, Etri J. 35 (4) p. 587, 2013, doi: 10.4218/etrij.13.1912.0025

[106] C.-C. Chueh, S.-C. Chien, H.-L. Yip, J. F. Salinas, C.-Z. Li, K.-S. Chen, F.-C. Chen, W.-C. Chen, A. K.-Y. Jen, *Toward high-performance semi-transparent polymer solar cells: Optimization of ultra-thin light absorbing layer and transparent cathode architecture*, Adv. Energy Mater. 3 (4) p. 417, 2013, doi: 10.1002/aenm.201200679

[107] M. Hiramoto, M. Suezaki, M. Yokoyama, *Effect of thin gold interstitial-layer on the photovoltaic properties of tandem organic solar-cells*, Chem. Lett. 3 (3) p. 327, 1990, doi: 10.1246/cl.1990.327

[108] J. Drechsel, B. Mannig, F. Kozlowski, M. Pfeiffer, K. Leo, H. Hoppe, *Efficient organic solar cells based on a double p-i-n architecture using doped wide-gap transport layers*, Appl. Phys. Lett. 86 (24) p. 244102, 2005, doi: 10.1063/1.1935771

[109] D. Wynands, M. Levichkova, K. Leo, C. Uhrich, G. Schwartz, D. Hildebrandt, M. Pfeiffer, M. Riede, *Increase in internal quantum efficiency in small molecular oligothiophene:C_{60} mixed heterojunction solar cells by substrate heating*, Appl. Phys. Lett. 97 (7) p. 073503, 2010, doi: 10.1063/1.3475766

[110] T. Moriarty, J. Jablonski, K. Emery, *Algorithm for building a spectrum for nrel's one-sun multi-source simulator*, Photovoltaic Specialists Conference (PVSC), 2012 38th IEEE Austin, Texas, USA, 2012 p. 001291 , 2012, doi: 10.1109/PVSC.2012.6317838

[111] R. Gresser, M. Hummert, H. Hartmann, K. Leo, M. Riede, *Synthesis and characterization of near-infrared absorbing benzannulated aza-bodipy dyes*, Chem-Eur. J. 17 (10) p. 2939, 2011, doi: 10.1002/chem.201002941

[112] J. Pina, J. Seixas de Melo, D. Breusov, U. Scherf, *Donor-acceptor-donor thienyl/bithienyl-benzothiadiazole/quinoxaline model oligomers: experimental and theoretical studies*, Phys. Chem. Chem. Phys. 15 (36) p. 15204, 2013, doi: 10.1039/c3cp52056k

[113] R. Schueppel, K. Schmidt, C. Uhrich, K. Schulze, D. Wynands, J. L. Bredas, E. Brier, E. Reinold, H.-B. Bu, P. Baeuerle, B. Maennig, M. Pfeiffer, K. Leo, *Optimizing organic photovoltaics using tailored heterojunctions: A photoinduced absorption study of oligothiophenes with low band gaps*, Phys. Rev. B 77 (8) p. 085311, 2008, doi: 10.1103/PhysRevB.77.085311

Author contributions

R.T., J.G. and M.R. conceived the idea. T. Mueller and D.W. fabricated devices while T.Meyer and R.T. carried out measurements at TUD under supervision of M.R. and K.L. Measurements at ISE were carried out by H.S. under supervision of J.H-E. and W.W. Measurements at TUe were carried out by A.F. and M.W. under supervision of R.A.J.J. Data analysis was performed by R.T. The manuscript draft was written by R.T., J.G. and H.S. The authors R.T., T.Meyer, J.G. H.S., T.M., R.A.J.J., M.R. and K.L contributed to revisions of the manuscript.

Acknowledgements

We would like to thank the Bundesministerium für Bildung und Forschung (BMBF) for funding parts of this work within the scope of the Innoprofile project 03IP602 and the OPEG project (13N9716).

Competing financial interests

The authors declare no competing financial interests.

Corresponding author

Correspondence to: R.A.J. Janssen (r.a.j.janssen@tue.nl) or K. Leo (leo@iapp.de)